

Strategies for Building Robust Traffic Networks in Advanced Energy Storage Devices: A Focus on Composite Electrodes


Yu Wang,* Xuwei Fu, Min Zheng, Wei-Hong Zhong,* and Guozhong Cao

The charge transport system in an energy storage device (ESD) fundamentally controls the electrochemical performance and device safety. As the skeleton of the charge transport system, the “traffic” networks connecting the active materials are primary structural factors controlling the transport of ions/electrons. However, with the development of ESDs, it becomes very critical but challenging to build traffic networks with rational structures and mechanical robustness, which can support high energy density, fast charging and discharging capability, cycle stability, safety, and even device flexibility. This is especially true for ESDs with high-capacity active materials (e.g., sulfur and silicon), which show notable volume change during cycling. Therefore, there is an urgent need for cost-effective strategies to realize robust transport networks, and an in-depth understanding of the roles of their structures and properties in device performance. To address this urgent need, the primary strategies reported recently are summarized here into three categories according to their controllability over ion-transport networks, electron-transport networks, or both of them. More specifically, the significant studies on active materials, binders, electrode designs based on various templates, pore additives, etc., are introduced accordingly. Finally, significant challenges and opportunities for building robust charge transport system in next-generation energy storage devices are discussed.

1. Introduction

Energy conversion and storage plays a more and more critical role in our daily lives due to the increasing and urgent interest on clean energy and technologies.^[1] Advanced batteries (e.g., lithium ion batteries (LIBs) and sodium ion batteries (SIBs)), capable of storing more energy and running much longer than conventional batteries, are, therefore, of great interests and have significant applications in numerous industries, such as

Dr. Y. Wang, X. Fu, M. Zheng, Prof. W.-H. Zhong
School of Mechanical and Materials Engineering
Washington State University
Pullman, WA 99164, USA
E-mail: yu.wang3@wsu.edu; katie_zhong@wsu.edu
Prof. G.-Z. Cao
Department of Materials and Engineering
University of Washington
Seattle, WA 98195-2120, USA

 The ORCID identification number(s) for the author(s) of this article can be found under <https://doi.org/10.1002/adma.201804204>.

DOI: 10.1002/adma.201804204

portable electronics, cell phones, electrical vehicles (EVs), aerospace, etc. For advanced batteries, higher and higher energy density and/or power density, long cycling stability, good device safety, and low-cost are the primary goals. Since the energy density is mainly dependent on the specific capacity and loading level of active materials (AMs), AMs usually dominate the volume and weight inside the batteries. Because of this, tremendous efforts have been focused on high-performance AMs. However, the electrochemical performance of energy storage devices (ESDs) is fundamentally determined by a collective contribution or teamwork of all the components: AMs, electrolyte, separator, conductive agent, binders, etc. More importantly, with the increasing interests on high-capacity AMs (e.g., silicon, sulfur, Li-rich cathode, etc.), it becomes very clear that the “traffic system” (i.e., the charge transport system) plays very critical roles in the performance of the high-capacity AMs. Take silicon anode for example, a durable and flexible conductive network inside the electrode composite has been

vital for addressing the big volume change issue. In this case, high-performance binders and conductive agent that can generate advanced conductive network are the keys.^[2] In addition, with the increasing interests on EVs and flexible electronics, building a powerful and robust charge transport system inside ESDs is an urgent and critical task to support fast charging/discharging capability and even flexibility of ESDs. In short, with the fast development of energy storage technologies, EVs, cell phones, etc., there is a critical, urgent, and challenging task on building powerful and durable charge transport system in next-generation advanced ESDs.

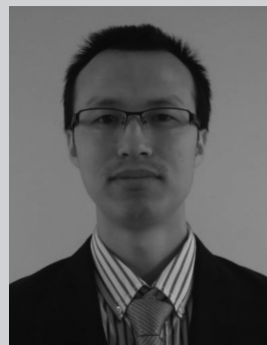
1.1. Charge Transport Inside ESDs

The thriving of big cities highly relies on a powerful traffic system that transports the people, foods, products, etc. Similar to this picture, ESDs are powered by the transportation of charges, including both ions and electrons. As illustrated in **Figure 1a**, one can analogize the charge transport system and AMs in the electrodes of ESDs to the traffic system and buildings (i.e., host system of people), respectively. This analogy example not only help to explain the relationship between

charge transport system and AMs in ESDs, but also is very instructive for a rational design of charge transport system that can support high energy density, high power density, long cycle stability and good safety. To further understand the charge transport inside ESDs, the flow of ions and electrons is illustrated by an in-series gear configuration as shown in Figure 1b. In this gear configuration, each gear corresponds to a unique part of the charge transport system. Specifically, the charge transport system is composed of several sections. Inside composite electrodes, there are four parts: ion transport network determined by the porous structures of the electrode composite, electron transport network built from the conductive agent and binder, the ion/electron transport inside the AMs, and the interfaces between conductive agents (electrolyte and conductive fillers) and AMs. Between the two electrodes, it is the ion transport network determined by the porous structures of the separator. At the same time, the connection between the gears represents the primary interfaces between the main components of ESDs. This configuration well reflects the collective nature of the charge transport. Every gear and the connection between two gears could be the limiting or dominant factor controlling the charges transport inside ESDs. As a result, the charge transport inside ESDs works in a similar way as the rotation of the gear configuration. In real ESDs, the input or output current is realized by countless in-series gear configuration as illustrated by Figure 1b.

1.2. Critical Factors Controlling the Charge Transport Networks

The work efficiency and stability of the charge transport system as illustrated by the in-series gear configuration are highly dependent on many and complicated factors. Although it is very hard to identify all the factors, the primary factors can be classified into about three categories as summarized in Figure 1c. The first category is the materials factors, including the ionic/electronic conductivities of the components and the material morphology (e.g., shape, size, etc.).^[3] The conductivities of battery materials are the most critical factor describing the charge mobility through the materials. The morphology of each component, primarily AMs or electrode particles, is another critical factor controlling the pathways for the ion/electron transport inside the battery materials.^[4–7] The second category is on interface factors that are the most complicated and also instable factors inside ESDs. This is fundamentally determined by the fact that an ESD is a combination of very different materials, including solid particles (active materials, conductive agent, etc.), organic liquids or inorganic/polymeric solids being as electrolyte, polymeric separator, binder, and metals as current collectors. Usually, there is no compatibility among these materials, which results in complicated interfaces. In Figure 1c, to name a few critical ones, the interfaces among the main components (AMs, electrolyte, separator, and conductive fillers) include the ones of separator/electrode, electrolyte/active material or solid electrolyte interphase (SEI),^[8,9] and conductive agent/active material. These interfaces correspond to the gear connection as illustrated in Figure 1b. It is clear that the connection quality of interfaces among these components/materials is one of the



Yu Wang received his B.S. and M.S. degrees in polymer science and engineering, Sichuan University, China. Then, he completed his Ph.D. in Prof. Zhong's group in 2015, Washington State University (WSU). He was an assistant research professor at WSU until August 2018. Now, he is a postdoctoral research associate at Oak

Ridge National Laboratory. His inspiration and passion for research is focused on functional polymeric nanocomposites, sustainable materials and technology, and manufacturing for energy storage and filtration applications.



Wei-Hong Katie Zhong is an endowed chair professor, Westinghouse Distinguished Professor, at Washington State University (WSU) in the area of polymer composites, biomaterials, and nanotechnology. She has served as a reviewer/panelist for NSF and DoE, and has been a consultant, collaborative researcher, and educator for the Boeing Company since 2006.



Guozhong Cao is Boeing-Steiner Professor of materials science and engineering, professor of chemical engineering, and adjunct professor of mechanical engineering at the University of Washington, Seattle, WA, USA. His current research is focused mainly on chemical processing of nanomaterials for solar cells, secondary

batteries, and supercapacitors, as well as actuators and sensors.

keys controlling the charge transport process.^[10,11] However, there is a big challenge to characterize and understand effects of these interface factors mainly due to the fact that the various interfaces are very complicated in structures and instable with time, temperature or electrochemical reactions.^[12–16] This is especially true for high-capacity electrodes with notable volume change.^[2,17–19]

The third category is summarized as configuration factors that describe the conductive network structures for ions/electrons transport. Based on the charge transport process as illustrated in Figure 1b, there are three different configuration

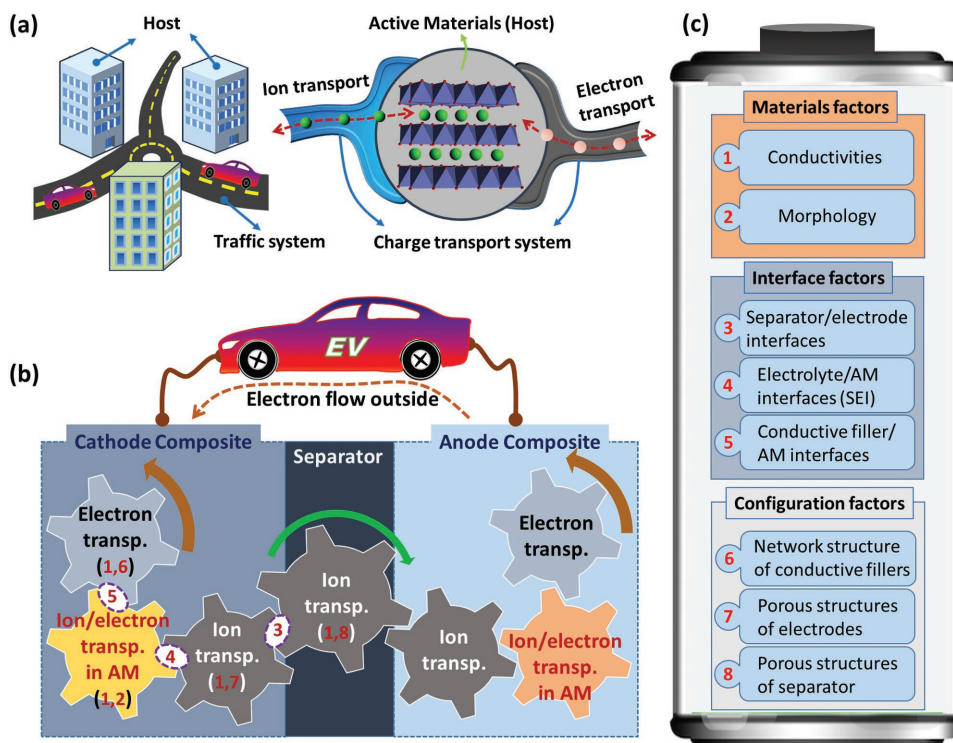


Figure 1. The charge transport system in a typical energy storage device (e.g. lithium-ion batteries) using liquid electrolytes. a) Analogizing the traffic system in cities to the charge transport system in battery electrodes. b) Illustration of the charge transportation process and its collective nature by in-series gear configuration. c) Classification of the main factors affecting the charges transport.

factors, including the electronic conductive network inside the electrodes, the pore network structures of the electrodes and the separator (i.e., the pathways for the ion transportation). Similar to the functions of veins in organisms, these configuration factors determine the 3D structures of pathways for charge transportation, which fundamentally control the charge transportation capability. Due to the complicated coupling effects among these factors, it is a big challenge to understand the relationships between these charge transport factors and the cell performance. In addition, environmental factors (e.g., temperature, applied deformation, vibrations) can notably affect the charge transport, which is not a focus discussed in this review.

1.3. Random Close Packing (RCP) for Conventional Composite Electrodes

In a traditional battery electrode, as illustrated in **Figure 2**, the charge transport system is built via several steps. For the first step, the conductive agent, polymer binder and AMs are mixed together in an appropriate solvent to form uniform electrode slurry. Then, the slurry is coated onto current collectors and a porous composite is fabricated after the solvent is removed. In this porous composite, the conductive agent “glued” by polymer binder constructs the electron transport network (ETN). This ETN will be further treated by heating and compression (i.e., calendaring) during the manufacturing of electrodes. At this

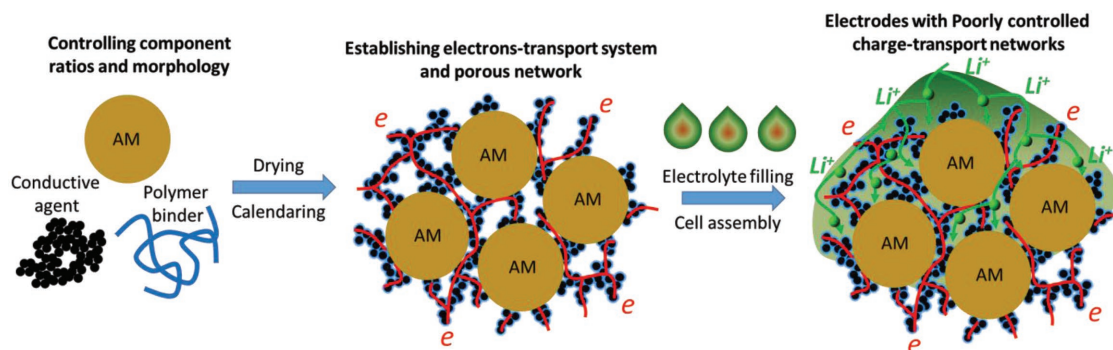


Figure 2. Illustration of the traditional strategy based on random close packing (RCP) for building the charge transport system in composite electrodes.

stage, the ion transport network (ITN) structure for ion transportation is also established by the porous structures of the dry composite electrodes. However, the ion transport system is not yet fully established as there are no mobile ions inside the electrode. At the next step, liquid electrolyte (e.g., organic liquid electrolytes) is introduced into the composite electrodes during the battery assembly. Through liquid wetting, all the porous structures of the composite electrodes and separator are occupied by the ion-conductive electrolyte, which finally establishes the ion transport system.

For this traditional strategy, each step and every component play an important role in building the transport networks. More specifically, the ratios among the components,^[20] the morphology of the AMs and conductive agents,^[21] the manufacturing conditions especially the calendaring process, etc.^[22] are the critical factors determining the final structures of the charge transport networks. In particular, electrode calendaring process has significant and complicated effects on the charge transport networks, and thus impacts the electrochemical performance. For the ITN (i.e., the porous structure of composite electrodes), the porosity (the volume fraction of ITN) is notably affected by the calendaring process.^[23,24] At the same time, the 3D structure of ITN (the tortuosity) is also notably affected by the calendaring process. For example, the tortuosity in the thickness direction usually increases with the reduction of thickness after calendaring.^[25–27] However, the thickness of the ITN is also reduced after calendaring, which shortens the travel distance for the Li-ions. For ETN, the calendaring can notably enhance the structure stability and network connectivity when combined with the effects of binder. This improvement helps to stabilize ETN and improve the electrochemical performance.^[23,24,28,29] In short, the calendaring is a simple process but a critical step for the quality control of composite electrodes. Owing to the simplicity and scalability, this RCP model has been widely employed by both industries and laboratories. At the same time, because most of the AMs are usually particles, this RCP strategy is the most important one in practice. As a result, it lays the foundation for other strategies as introduced in this review. The main disadvantage for this traditional strategy is the poor controllability over the structures and properties of the transport networks. The random self-packing of electrode components is sensitive to many factors, such as the characteristics of components, ratios, manufacturing conditions, etc. Therefore, the primary goal of the strategies summarized here is to achieve better control over the charge transport networks.

1.4. Scope and Structure

As introduced above, the whole picture of the charge transport system consists of two sub-systems including the physical networks (similar to roads in a real traffic system) and the conduction media (the ion-conductive electrolyte and electron-conductive agents). At the same time, it can be physically divided into about six sections as illustrated in Figure 1b. Therefore, a comprehensive summary of the related efforts and understanding of the whole picture will be an extremely huge and challenging task. In this review, for clarity, we try to focus

on the physical networks of the most important two sections in composite electrodes: the ion and electron transport networks surrounding the AMs. The main reason for such reviewing is explained below. It is well accepted that, with the increasing demands for higher energy and power densities, long cycle life and safety, building robust physical networks for efficient ions/electrons transport in composite electrodes becomes increasingly critical, especially for high-capacity AMs. High-capacity AMs, such as sulfur and silicon, are well known by their huge volume change during the electrochemical reaction processes, which result in serious structural instability for the charge transport system.^[30–32] Therefore, building advanced physical network structures for transport of both ion and electron is one of the most critical tasks for the success of high-capacity AMs. Therefore, other sections of charge transport system, such as the ion/electron transport inside AMs, the ion/electron transport through the interfaces (such as solid-electrolyte-interphase), and the ion transport through the separator are not included here. Meanwhile, the effort on improving conductivity of conductive media (e.g., electrolyte and conductive fillers) is not included in this review either.

In the following sections, we will organize the main strategies into three categories based on their contribution to different part of the charge transport networks as shown in **Scheme 1**: 1) strategies for mainly controlling ITN, 2) strategies for mainly controlling ETN, and 3) strategies for controlling both ITN and ETN. Although this organization is not technically rigorous since ETN and ITN are coupled somehow, it will help the understanding of their roles as discussed in this review.

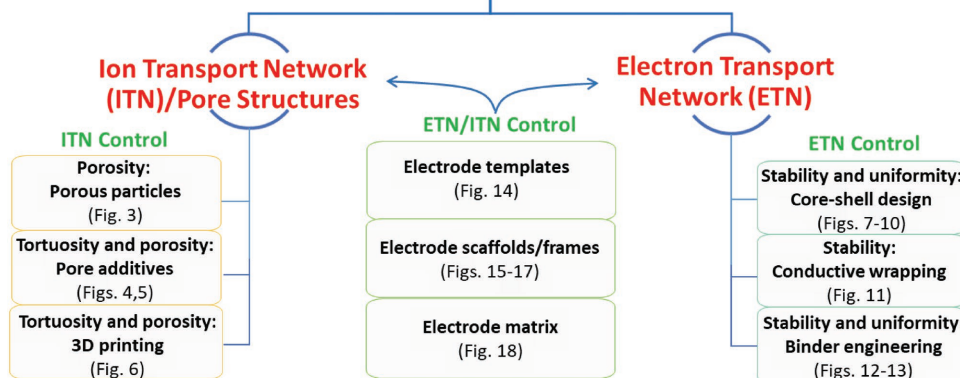
2. Controlling ITN in Composite Electrodes

For an ESD with liquid as the electrolyte, the ITN is actually the porous network inside the composite electrodes. Therefore, the strategies for ITN control are the ones controlling the porous structures of the composite electrodes. In practice, the porous structure in composite electrodes is a product of the teamwork by all the components and the manufacturing process. Thus, it is hard to control the whole ITN via a simple and single step. It is noted that the component ratios and manufacturing conditions (e.g., calendaring processing as introduced above) are critical factors determining both the ITN and ETN structures; however, we will not emphasize them here and the readers are suggested to read the review by Ein-Eli and co-workers.^[22]

2.1. Porous Particles: Porosity Control for ITN

Since AM is the dominate component inside the composite electrodes, design of AMs with rational morphology facilitating fast ions transport is one primary way to control the ITN structure. A good example of this point is the work on porous AMs.^[34–50] For electrodes with porous AMs, the structures of ITN will include two parts: one is the porous structures around the AMs; and the other is the porous structures inside the AMs. For example, as shown in **Figure 3a,b**, Cao and co-workers reported a facile strategy based on amorphous TiO₂/oleylamine nanoprecursor

Charge Transport Networks in Composite Electrodes



Scheme 1. Overview of the strategies summarized in this review for controlling the charge transport systems in composite electrodes.

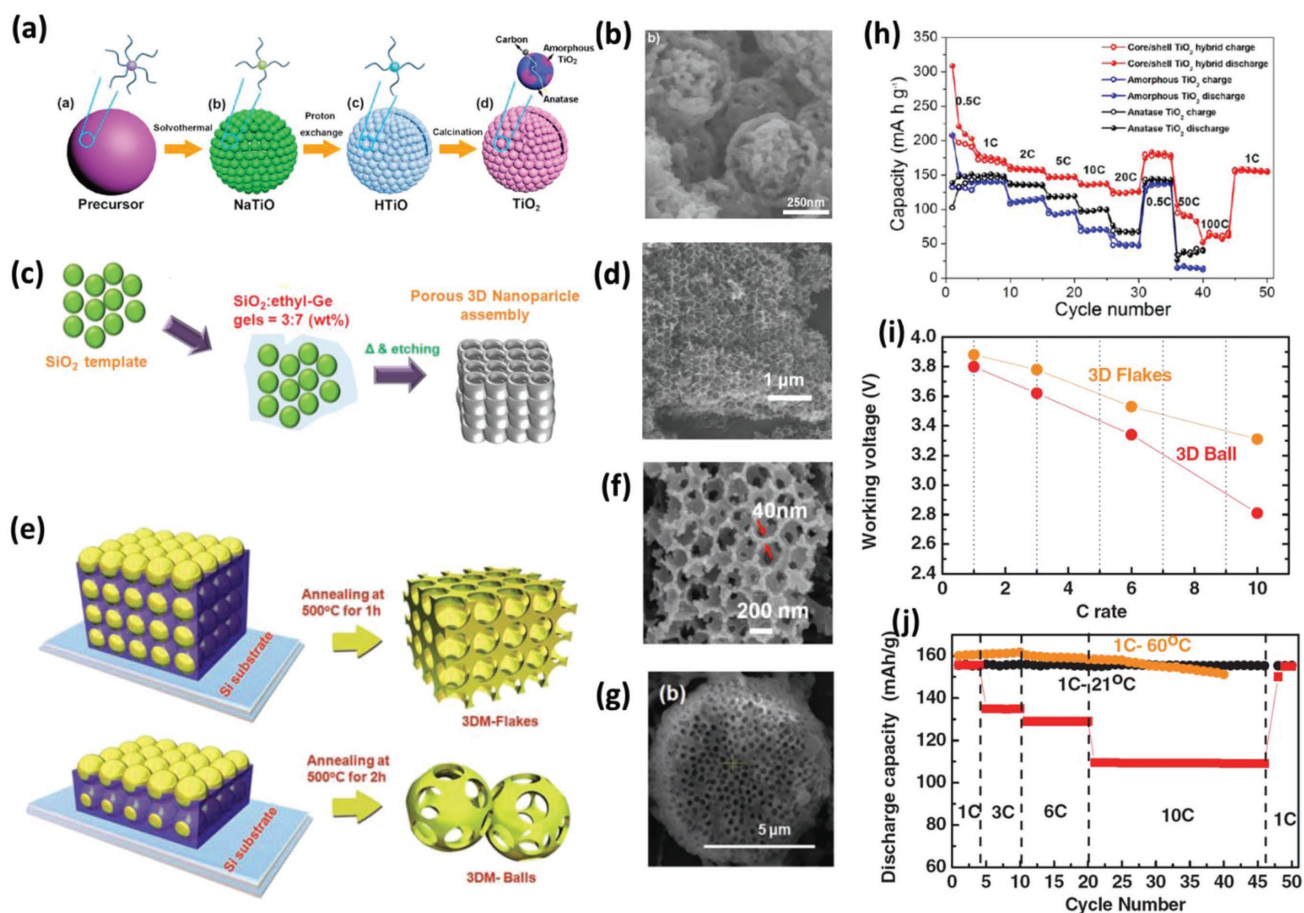


Figure 3. Porous particle engineering for building fast ion-conduction channels inside active materials (AMs). a,b,h) Porous TiO_2 particles by self-assembly: a) Schematic of the synthesis strategy based on an oleylamine-assisted self-assembly process. b) SEM image of the porous TiO_2 particles. h) C-rate performance. c,d) 3D porous Ge particles by HF etching: c) Schematic of the fabrication strategy based chemical etching of silica template. d) SEM image of the 3D porous Ge particles. e–g,i,j) 3D porous LiMnPO_4 (LMP) flakes and micro-ball: e) Illustration of the strategy by poly(methyl methacrylate) (PMMA) template method. f,g), SEM images of the porous LMP flakes and balls, respectively. i,j) C-rate and cycle performance for the 3D porous LMP flakes and micro-ball. a,b,h) Reproduced with permission.^[33] Copyright 2017, American Chemical Society. c,d) Reproduced with permission.^[34] Copyright 2010, Wiley-VCH. e–g,i,j) Reproduced with permission.^[35] Copyright 2011, Wiley-VCH.

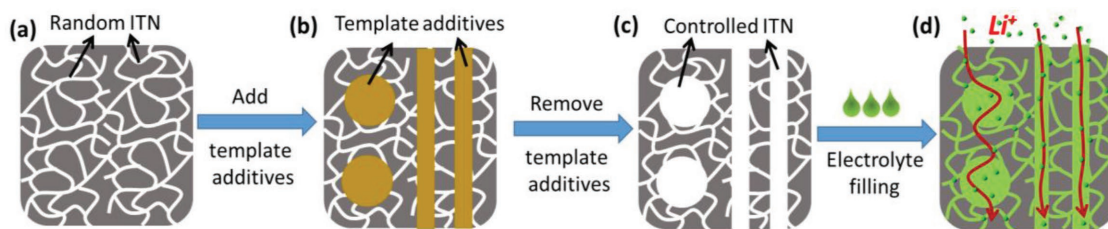


Figure 4. Illustration of template additive strategy for building controllable ion-transport-network (ITN) in composite electrodes. a) Conventional porous composite electrodes with random ITN; b) porous composite electrodes with template additives; c) porous composite electrodes with controlled ITN after the removal of template additives; d) establishing fast ions transport system based on controlled ITN.

for fabrication of porous core-shell TiO_2 particles as advanced anode for LIBs.^[33] In this strategy, the porous structure of the TiO_2 particles was controlled by a self-assembly process of a nanoprecursor. This self-assembly method has been widely used to prepare porous microparticles, such as pomegranate-inspired porous Si particles by Cui and co-workers.^[42] Chemical etching is another important conventional method to prepare porous AM.^[51–54] For example, Cho and co-workers reported different types of 3D porous germanium nanoparticle assemblies as high-performance anode for LIBs.^[34] In this strategy, silica NPs were employed as the template of the pores. With the help of assembly and chemical etching of silica by HF (see Figure 3c), 3D porous germanium particles were fabricated (see Figure 3d). Cho and co-workers reported a similar strategy for fabrication of macroporous silicon particles by metal-assisted chemical etching.^[37] They employed commercially available bulk Si powders with size of about 10 μm as the raw materials, and successfully fabricated 3D porous Si particles with nanoscale pores.

In addition, strategies on fabrication of porous cathode particles are also of great interest.^[35,44,45,49,55] For example, Cho and co-workers reported a polymer-template method to prepare porous LiMnPO_4 (LMP) flakes and microball as shown in Figure 3e.^[35] In this strategy, poly(methyl methacrylate) (PMMA) colloidal crystals were used as the template for the pores, which can be removed easily by an annealing process. The scanning electron microscopy (SEM) images (see Figure 3f,g) indicate that the pores were well controlled by the template with a size of ≈ 250 nm. Pores were also introduced into AMs with different shape, such as porous nanosheet,^[50,56] porous nanofiber^[33] and meshed plate-like particles.^[57] For a more comprehensive summary on porous AMs, the readers are suggested to read the review by Stein and co-workers.^[49]

The pores inside AM particles can significantly improve the charge transport by mainly three mechanisms: 1) opening more pathways for fast ions transportation, 2) reducing the diffusion distance of charges inside the AM particles, and 3) stabilizing the structures of high-capacity AMs during volume change. As a result, the C-rate capability can be improved as shown in Figure 3h–j. In particular, the porous assembled TiO_2 delivered a specific capacity around 150 mAh g^{-1} even at a high current density of 20 C, which is about 3 times of the nonporous TiO_2 particles as shown in Figure 3h.^[33] For the porous LMP flakes and microball, Cho and co-workers found that 3D porous flakes delivered much higher capacity at different C-rates as compared with 3D porous balls as shown in Figure 3i,j. As shown above, porous design of AMs is an effective strategy of adjusting the

ITN structures. However, it will inevitably reduce the energy density due to the increase of pore volume. At the same time, there is little knowledge on how the porous structures affect the mechanical and structural stability of AMs and the final electrode composites, which may have notable influence on the performance stability. Therefore, more fundamental studies on the structure-properties-performance relationships are in critical need for this porous AM strategy.

2.2. Pore Additives: Porosity and Tortuosity Control for ITN

For particles-based electrodes, the ITN around the AMs can be controlled by addition of template additives. Similar to the template methods employed for creating porous structures inside AMs, template additives generate well-defined pores inside composite electrodes after their removal as illustrated in Figure 4. In this strategy, the template additives are introduced as an additional component to form well-defined pore template. Depending on the properties and structures, the template additives can form ordered or nonordered pores after removal. Usually, they are removed after the calendaring process in order to protect the ITN that was already created by the template additives.

Magnetized Rods as Pore Additives Creating Ordered ITN: There are several types of template additives reported thus far. The first one is magnetic template additives. This type of template additives was initiated by Chiang and co-workers.^[58] As illustrated in Figure 5a, magnetized nylon rods are first introduced into the electrode slurry. With the help of magnetic field, these nylon rods align with the magnetic field and form ordered structure inside the composite electrodes. After a step of consolidation, the aligned nylon rods were removed by pyrolysis. As a result, ordered porous structures can be realized. Figure 5b,c shows the SEM images of the fracture surface for the electrode composite with aligned nylon rods before and after the removal of template additives. The aligned structures along the thickness direction are clearly shown. The most significant contribution of the aligned pores is the fast ion transport in thick electrodes. They successfully demonstrated a thick electrode with thickness around 700 μm and an areal capacity above 12 mAh cm^{-2} , which is about three times of the commercial LIBs. The aligned pore structure significantly improved the ion transport in the thick electrode. As a result, it notably improved the C-rate performance, especially at high C-rates, such as 1 C, as shown in Figure 5d.

Salts as Pore Additives for ITN Control: Salts, such as table salt, were employed as template additive to create pores inside

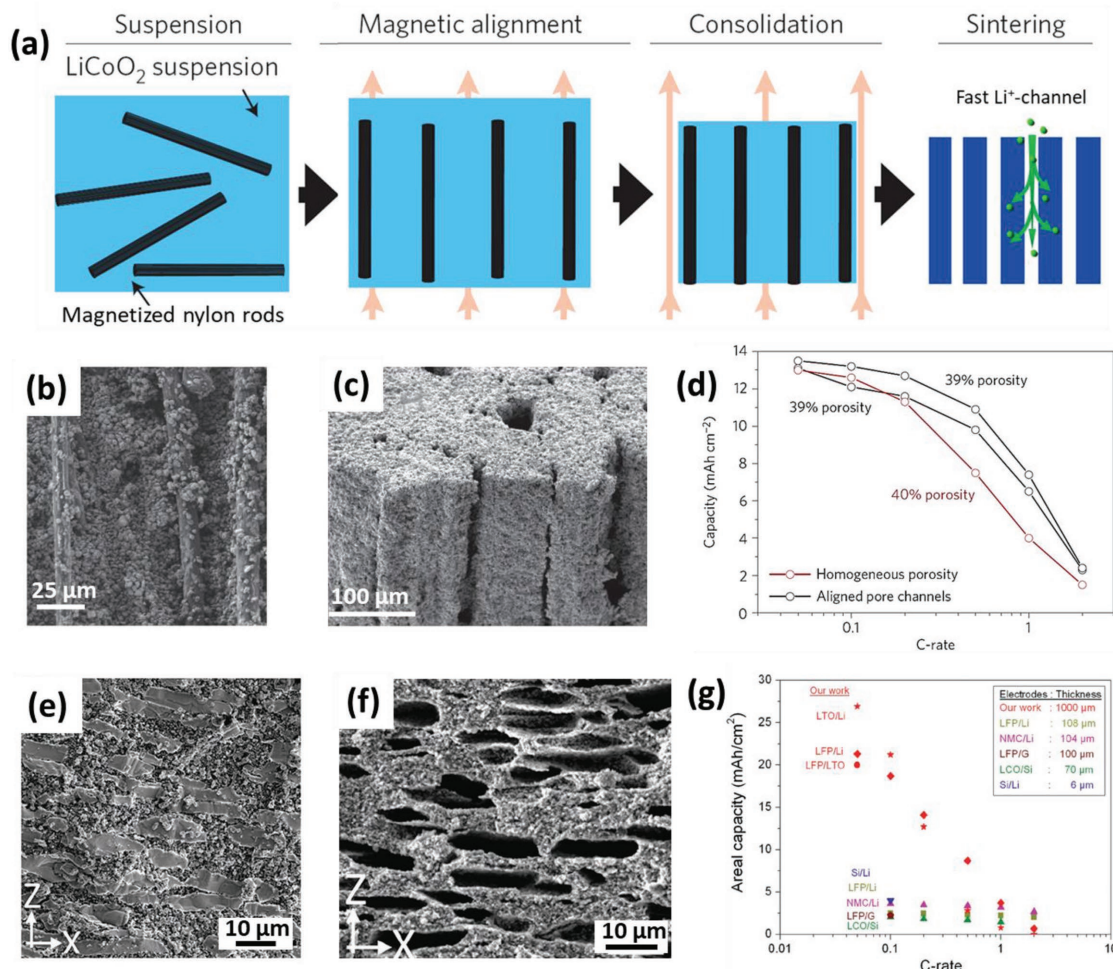


Figure 5. Template additives strategy for building fast and controllable ITN in composite electrodes: a–d) Magnetized polymer rods as template additives to build ordered pores in thick composite electrodes: a) Schematic of the fabrication process. b,c) SEM images of the fracture surface for thick composite electrodes before and after the removal of the magnetized nylon rods. d) C-rate performance comparison between thick composite electrodes with aligned pore channel and conventional porous structures. e–g) Salt crystals as template additives to build controlled pores in thick composite electrodes: e,f) SEM images of the fracture surface for a thick electrode composite before and after the removal of table salt (NaCl) crystal. g) C-rate performance comparison for thick composite electrodes with salt-templated pores and conventional porous structures. a–d) Reproduced with permission.^[58] Copyright 2016, Springer Nature). e–g) Reproduced with permission.^[59] Copyright 2018, Wiley-VCH.

composite electrodes.^[59–61] For example, Liu and co-workers reported the first study on using sacrificial NaCl to introduce controlled pores in a Si-based electrode. They successfully demonstrated an areal capacity of $\approx 4 \text{ mAh cm}^{-2}$ at a C/10 rate.^[61] Similar to this idea, Seznec and co-workers further developed a method by combination of salt-template and spark plasma sintering for fabrication 1 mm thick porous LiFePO₄ (LFP) and Li₄Ti₅O₁₂ (LTO) composite electrodes.^[59] They directly mixed the NaCl particles as templating agent with carbon-coated AMs (LFP or LTO). After sintering, the AMs and NaCl particles formed a binder-free composite as shown in Figure 5e. The NaCl particles were then removed by DI-water and pores were controlled as shown in Figure 5f. Via this template additive method, they demonstrated a very thick electrode composite ($\approx 1 \text{ mm}$ for the thickness) for both LFP cathode and LTO anode with a controlled porosity around 40%. Benefited from the controlled porous structures, they demonstrated a full battery with specific areal capacity

of 20 mA h cm^{-2} , which is ≈ 4 times higher than conventional Li-ion batteries (4 mA h cm^{-2}). This battery also showed much improved C-rate performance (see Figure 5g). As introduced above, pore additives provide a very facile way to generating controllable pores inside the electrode composites. It is effective to adjust both the porosity and tortuosity of ITN. This strategy is very promising for the fabrication of thick electrodes with well-defined ITN configuration to achieve higher energy and power densities. For future studies, the morphology of pore additives needs to be further optimized with the help of simulation studies that can predict the best pore configuration for thick electrodes.

2.3. Additive Manufacturing for Programmable ITN

Building programmable ITN in composite electrodes by new manufacturing technology, such as 3D printing, represents

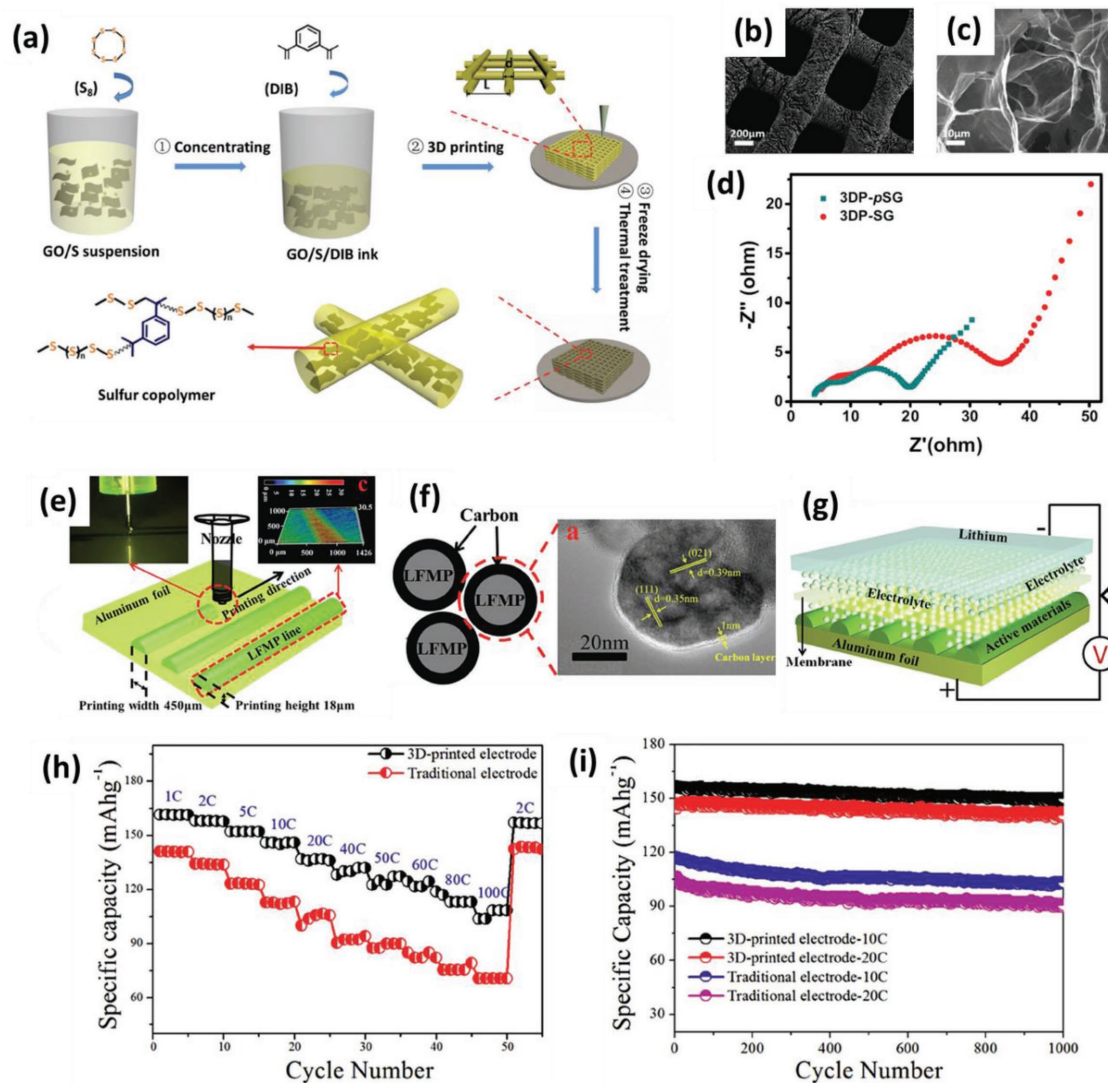


Figure 6. 3D printing for building programmable ITN in composite electrodes. a–d) 3D printing of a sulfur–graphene composite cathode for Li–S batteries: a) Illustration of the fabrication process and strategy. b, c) SEM images of the printed cathode and sulfur–graphene composite. d) Electrochemical impedance spectra (EIS) comparison of 3DP-pSG and 3DP-SG after 50 cycles. e–i) 3D printing of LiMn_{1-x}Fe_xPO₄ nanocrystals based electrodes for improved C-rate performance: e) Illustration of the 3D printing fabrication process. f) Structures of the carbon-coated LiMn_{1-x}Fe_xPO₄ as the active material. g) Illustration of the cell configuration assembled with the 3D-printed electrode. h, i) C-rate capability and cycle performance comparison between the 3D-printed and traditional electrodes, respectively. a–d) Reproduced with permission.^[62] Copyright 2017, Wiley-VCH. e–i) Reproduced with permission.^[63] Copyright 2016, Wiley-VCH.

another attractive strategy for the control of ITN. With the increasing interest on customizable products, 3D printing is of great interest for the fabrication of advanced LIBs,^[62–70] and redox flow batteries.^[71–73] For example, Yang and co-workers recently reported a 3D printed sulfur cathode for Li–S battery.^[62] The process is illustrated in **Figure 6a**. First, the authors designed a printable ink, which was composed of sulfur particles, 1,3-diisopropenylbenzene (DIB), and condensed graphene oxide dispersion. Via an extrusion-based 3D printing approach, they printed a sulfur copolymer–graphene composite electrode with well-defined periodic microlattices. The pore size of the microlattices is around 500 μm as shown in **Figure 6b**. At the same time, small pores with size around

30 μm were formed inside the printed electrode as shown in **Figure 6c**. This hierarchical porous structure notably reduced the resistance of the cell (see **Figure 6d**), indicating a faster ion transport in the ITN defined by the 3D printed architecture. Another example is a 3D-printed cathode based on LiMn_{1-x}Fe_xPO₄ (LMFP) nanocrystals reported by Pan and co-workers.^[63] As shown in **Figure 6e–g**, in this study, the authors employed carbon-coated LMFP nanoparticles as the AM and printed the electrode with width around 450 μm and height of 18 μm . The alignment of the semi-circle electrode solid lines actually creates a gradient pore space between them, which helps the ion transport as shown by the C-rate performance in **Figure 6h**. They demonstrated a high capacity of $\approx 120 \text{ mAh g}^{-1}$

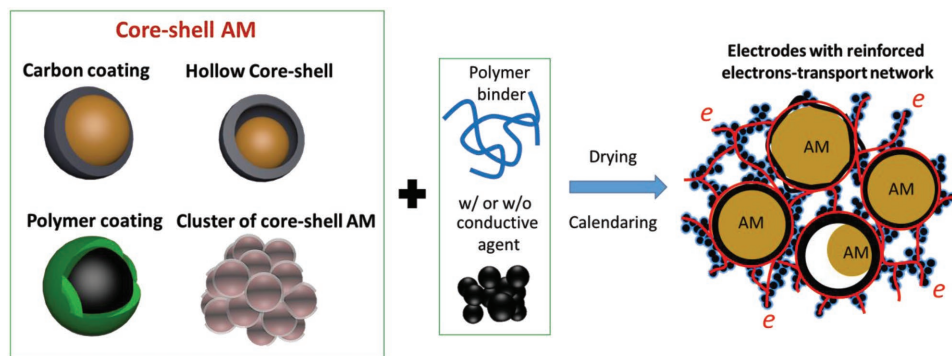


Figure 7. Enhancing and stabilizing the electron-conductive-network (ETN) in composite electrodes by various core–shell designs of active materials.

@ 100 C for LMFP electrode, which is about two times of that for the electrodes fabricated by traditional slurry casting methods. At the same time, excellent structural stability and cycle stability was also realized for the 3D printed LMFP electrode (see Figure 6i). As an attractive manufacturing method, 3D printing provides a programmable way to control the microstructures of electrode composites. Theoretically, it can realize the best control over ITN or ETN, and enable the fabrication of microbatteries and micro-supercapacitors.^[70,74–76] Obviously, 3D printing is very promising for the fabrication of small ESDs with well-defined structures. However, this indicates it is not suitable for large-scale fabrication. At the same time, there are many requirements for the electrode inks to be printable. All these factors limit the broad applications of 3D printing in energy storage technology, which should be considered in the future studies.

3. Controlling ETN in Composite Electrodes

It is well known that most of the AMs, especially the ones with high capacity (e.g., LiMO_2 ($M = \text{Ni, Mn}$) oxides, LiFePO_4 , $\text{LiNi}_x\text{Co}_y\text{Mn}_{(1-x-y)}\text{O}_2$, silicon and sulfur, etc.), are poor in electronic conductivity as compared with conductive agents (e.g., carbon-based nanofillers), although some of them are actually electronically conductive.^[77–79] Due to this fact, building a robust conductive network around the AMs is one of the primary tasks to realize powerful and durable electron transport inside the composite electrodes. Traditionally, conductive agents, such as carbon black, are simply mixed with a polymer binder to build the ETN as illustrated in Figure 2. Although this traditional strategy has been widely used today, there are several drawbacks. First, it is difficult to achieve uniform electronic/ion contacts between conductive agents and active materials due to a nonuniform distribution of components. Second, the electronic contact is not stable owing to insufficient adhesion. These two drawbacks do not only limit the capacity extraction of AMs, but also cause fast capacity fading due to the interface instability.^[80–82] This situation becomes even worse for the high capacity active materials with notable volume change during cycling, such as silicon and sulfur.^[30,83,84] Therefore, strategies on building deformation-tolerant and strong ETN in composite electrodes with high-capacity AMs are in critical need for the success of high-capacity AMs.

3.1. Core–Shell Design of AMs: Uniform and Stable Electronic Contact

Core–shell strategy has been widely employed to build uniform and stable electronic contact between AMs and conductive agents. In this configuration, the AMs usually are the core, and the nanostructured conductive agents act as the shell. As illustrated in Figure 7, there are several types of core–shell structures: carbon coated AMs, conductive polymer coated AMs, hollow core–shell structure, clusters of core–shell AMs. It should be noted that there are many other functions for the conductive shell in addition to the electron conduction. For example, it can protect the AM from dissolution (such as sulfur),^[85,86] or help to stabilize the solid-electrolyte-interphase (SEI) for silicon, etc.^[87–92] To build the final ETN in composite electrodes, core–shell AMs can be either directly sintered, or mixed with polymer binder and/or additional conductive agents. In both cases, the conductive shell helps to build a robust ETN for uniform and stable electron transport. In the following, we will focus on two types of conductive coating methods for fabrication of core–shell AMs.

Carbon-Coating for Core–Shell AMs (Carbon@AM): Conductive carbon coating of electrode particles has been extensively studied recently to enhance the electron-conduction and so the performance.^[19,93,96–109] Carbon@AM is probably the most effective way to control the ETN structures. With this carbon shell, the uniformity and stability of electron/ion transfer into or outside the AMs can be remarkably improved. There are several ways for the fabrication of carbon@AM. The first example is thermolysis.^[90,110,111] For this strategy, the AMs are first coated by a precursor (e.g., polymers or small organic molecules) in a liquid, then the mixture is treated at high temperatures to carbonize the precursors.^[112] This thermolysis-based technique is usually suitable for electrode materials with high melting point, such as $\text{Li}_4\text{Ti}_5\text{O}_{12}$,^[93,113] silicon,^[19,105,114,115] LiFePO_4 ,^[94,116,117] etc. As shown in Figure 8a–d, one can find that the thickness of the carbon nanocoating is usually very small (e.g., less than 10 nm), which can ensure a low resistance for Li^+ transfer. Carbon nanocoating is applicable for electrode materials with different morphology from 0D particles (Figure 8b), 1D rod (Figure 8a), and fibers (Figure 8c) and 2D plates (Figure 8d). As introduced previously, the carbon nanoshell has multiple functions in addition to reinforcing ETN structures/properties. For example, for $\text{Li}_4\text{Ti}_5\text{O}_{12}$, carbon coating can significantly

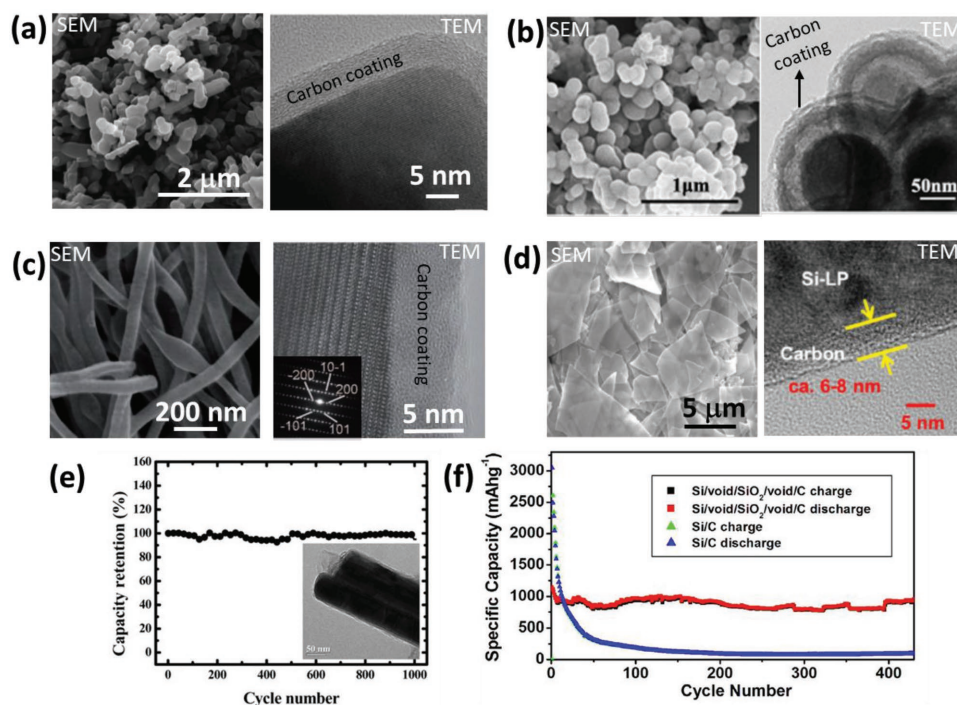


Figure 8. Conductive carbon coating for ETN control in composite electrodes. a,e) Carbon-coated Li₄Ti₅O₁₂ nanorod: a) SEM and TEM images, and e) cycle stability, of the carbon-coated Li₄Ti₅O₁₂ nanorod. b,f) Carbon and silica double coated Si anode: b) SEM and TEM images, and f) cycle stability of the carbon and silica double-coated Si anode. c) Carbon-coated LiFePO₄ nanowires by electro-spinning method. d) Carbon-coated Si thin flakes. a,e) Reproduced with permission.^[93] Copyright 2010, The Royal Society of Chemistry). b,f) Reproduced under the terms of the CC-BY Creative Commons Attribution 4.0 International License.^[91] Copyright 2015, Springer Nature. c) Reproduced with permission.^[94] Copyright 2011, Wiley-VCH. d) Reproduced with permission.^[95] Copyright 2012, The Electrochemical Society of Japan.

improve the C-rate performance,^[99,118] cycle stability as shown Figure 8e,^[93] and stability with electrolyte.^[119,120] For big-volume-change electrode particles (e.g., silicon), carbon coating is also critical for stabilizing the ETN structures and SEI layer.^[87–89,92,110,121] However, it should be noted that for silicon, carbon-coating is usually combined with a rational design of pore structure inside the particles to compensate the big volume change. Figure 8f is an example by Xia and co-workers which shows a much improved cycle stability for a carbon coated Si/void/Silica anode.^[93]

Conductive Polymer Nanocoatings for Core–Shell AMs: Similar to the carbon nanocoating, conductive polymers are also of great interest for fabrication of core–shell AMs. As a result, different types of conductive polymers have been studied as summarized in Figure 9. These conductive polymers include PEDOT:PSS,^[85,122,124–126] polypyrrole (PPy),^[123,127–133] Polyaniline (PANI),^[126,134–137] etc. Different from carbon-coating, conductive polymer coatings are believed to be more flexible in terms of mechanical properties and applicable to various electrode materials. For example, conductive polymer coating was employed for both high-melting-point electrodes (e.g., silicon,^[122,125] LiFePO₄^[128]) and low-melting-point electrodes (e.g., sulfur^[85,138,139]). Since conductive polymers are relatively more flexible than carbon materials, they are more attractive for high-capacity electrode materials experiencing notable volume change during charging and discharging. Figure 9a is an example by Coleman and co-workers who directly employed PEDOT:PSS as both binder and conductive coating for Si-NPs anode.^[122] As shown by the SEM image, PEDOT:PSS can

form a uniform coating onto Si-NPs and build a robust polymeric ETN for the Si anode. PPy is another classic conductive polymer material that has been frequently employed to fabricate core–shell AMs.^[131,133,140,141] Due to the good processing properties of PPy, it can enable the fabrication of core–shell nanowires as shown by Figure 9b, which is about a type of PPy@V₂O₅ nanofabric reported by Mao and co-workers.^[123] In a more systematic study, as shown in Figure 9c,d, Cui and co-workers compared the performance of sulfur cathodes with different types of conductive polymer coatings and found that PEDOT:PSS is the best option for sulfur cathode.^[85] In addition to electron conduction, another advantage by using conductive polymer is the good binding function. In other words, conductive polymers can be employed as both conductive agent and binder materials for battery electrodes. This is significant for battery electrodes since it can help to increase the overall loading level of active materials, and thus increase the energy density of the final battery.

Similar to core–shell carbon@AM, conductive polymer@AMs also demonstrated much improved electrochemical performance in terms of C-rate capability and cycle stability. For example, as shown in Figure 9e, PEDOT:PSS coating notably improved the C-rate performance of Si-NP anode even without the design of pore inside the Si-NPs. The big volume change of Si-NPs did not cause fast capacity decay in the first couple of cycles for this PEDOT:PSS@Si-NP anode. This is probably due to much better mechanical flexibility for conductive polymers as compared with carbon-coating. The type of conductive polymer coatings also has a significant impact on the electrochemical

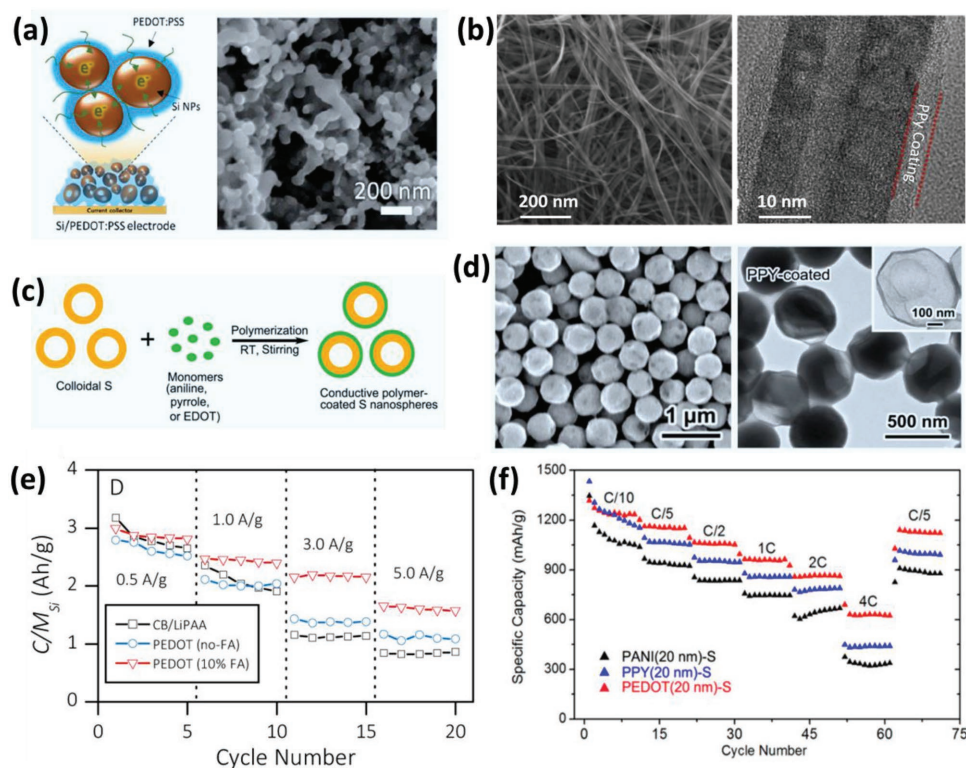


Figure 9. Conductive polymer coating for ETN reinforcement. a,e) PEDOT:PSS-coated Si nanoparticles for stabilizing ETN: a) Schematic and SEM image of the PEDOT:PSS-coated Si-NPs, and e) C-rate performance for the conductive polymer coated Si-NPs. b) Polypyrrole-coated V₂O₅ nanofibers. c,d,f) Conductive-polymer-coated sulfur particles for Li-S batteries: c) Schematic of the fabrication strategy. d) SEM and TEM images of PPy-coated S-NPs. f) C-rate capability for the S-NPs with different conductive polymer coatings. a,e) Reproduced with permission.^[122] Copyright 2016, American Chemical Society. b) Reproduced with permission.^[123] Copyright 2015, Elsevier. c,d,f) Reproduced with permission.^[85] Copyright 2013, American Chemical Society.

performance as revealed by Cui and co-workers in Figure 9f. They found that, among the three conductive polymers (PPy, PANI, and PEDOT:PSS), PEDOT:PSS gave rise to the best electrochemical performance, including C-rate and cycle stability. They explained this finding as the results of a higher binding energy between PEDOT:PSS and polysulfides, as compared with other two conductive polymers.

Encapsulation for Hollowed Core-Shell AMs: Encapsulation is widely used to prepare special hollowed core-shell structure for especially high-capacity active materials, such as silicon,^[142–147] sulfur,^[148–155] and aluminum.^[156] The hollow structure can reduce the damage to the conductive network structures during volume change. There are several encapsulation methods. One classic method for Si-anode is chemical etching as shown Figure 10a, which was reported by Li et al.,^[157] and Fan and co-workers.^[158] For this method, the active materials are coated with two types of materials in sequence: sacrificing coating and conductive coating. The sacrificing coating is finally removed by chemical etching, forming the hollow structure inside the core-shell particles. For Si anode, the sacrificing coating is usually silica that can be easily removed by HF acid. Figure 10b is a transmission electron microscopy (TEM) image for the hollow C@Si particles prepared by this method.^[158] Similar to chemical etching, electroless etching, i.e., etching the active materials directly for creating free space inside the core-shell AMs, was reported by Cho and co-workers.^[159] Another method is infusion of active materials into hollow conductive agents, such as carbon

nanofibers^[154] or nitrogen-doped carbon nanofibers as shown in Figure 10c,d.^[160] For this method, the active material (e.g., sulfur) is melted and infused into the hollow host. Clearly, hollow core-shell AMs provides another effective solution to build stable ETN for especially big-volume-change AMs. With this hollow core-shell AMs, the electrochemical performance and its cycle stability have been notably improved for both Si-anode (Figure 10e) and sulfur-cathode (Figure 10f). The excellent cycle stability for the hollow C@Si (see Figure 10e) also indicates that the carbon-shell can stabilize the SEI. For the core-shell sulfur composite with carbon nanofibers, the improved specific capacity and cycle stability may also indicate that 1D carbon nanofibers can help to build stable ETN due to the entanglements of nanofibers.

3.2. Let It Expand: Deformation-Tolerant ETN by Conductive Wrapping

Conductive wrapping by usually flexible 2D nanomaterials, such as graphene, is another important strategy for building robust and flexible ETN in composite electrodes. Flexible or expandable ETN is especially critical for the success of high-capacity electrodes, such as silicon and sulfur, since the volume change is so big ($\approx 300\%$ for Si) that the ETN may be destroyed after several cycles of shrinking and expanding.^[80,83] Therefore, to address this challenge, the hollow core-shell structures as introduced above, and conductive wrapping of AMs are

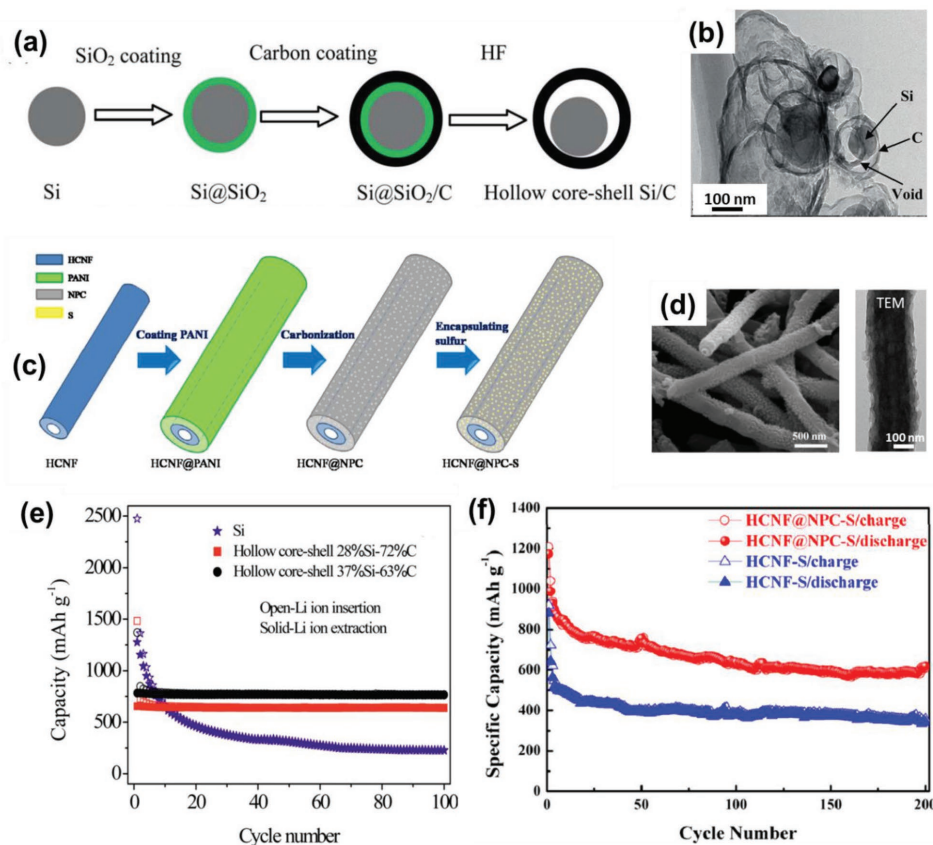


Figure 10. Hollow core-shell AMs for ETN stabilization. a,b,e) Hollow C@Si particles for stabilizing ETN around Si: a) Schematic of the fabrication strategy based on a combination of carbon coating and chemical etching. b,e) TEM image and electrochemical performance of the hollow C@Si particles. c,d,f) Hollow encapsulation of sulfur in carbon nanofiber. c) Schematic of the fabrication strategy based on carbonization of PANI nanofiber and sulfur infusion. d) SEM and TEM images of the encapsulated sulfur in carbon nanofiber. f) Electrochemical performance of the encapsulated sulfur in carbon nanofiber. a,b,e) Reproduced with permission.^[158] Copyright 2014, The Royal Society of Chemistry. c,d,f) Reproduced with permission.^[160] Copyright 2014, Elsevier.

of great interest for high-capacity electrode materials. The most popular nanomaterials employed for flexible conductive-wrapping (FCW) is graphene or reduced graphene oxide (rGO).^[163–172] This strategy has been widely used for especially silicon^[167,173,174] and sulfur,^[166,169,175–177] and also conventional electrode materials, such as LiFePO₄,^[178] LiMnO₂.^[179] Graphene is a 2D atomic film with high conductivities, excellent flexibility and mechanical strength. At the same time, graphene itself tends to wrap up to form loose structures due to its high surface energy. These features make it an ideal nanomaterial for flexible or expandable wrapping. To achieve good wrapping structures, surface treatment of both graphene and active materials is usually required in order to create sufficient interactions driving the wrapping process. For example, by the help of a polyelectrolyte (PDDA), Guo and co-workers reported a simple wrapping strategy based on electrostatic interactions to fabricate rGO wrapped Si nanoparticles (Figure 11a).^[161] The SEM and TEM images (see Figure 11b,c) clearly show the wrapped Si-NPs by rGO sheets. These rGO wrapped Si finally built a flexible conductive ETN, which notably improved the cycle stability (see Figure 11d). Similarly, Zhang et al. reported a type of rGO wrapped sulfur for Li-S batteries (Figure 11e–g).^[162] This rGO wrapping not only provided a flexible ETN for nonconductive sulfur, but also acted a barrier layer to block the diffusion of

polysulfides. As a result, they achieved a high specific capacity above 500 mAh g⁻¹ even at 4C (Figure 11h). Another method was reported by Cui and co-workers, by which they created graphene-wrapping onto sulfur nanoparticles using PEG as mediator.^[176] For these high-capacity active materials, flexible and conductive wrapping not only address the conductivity issue of high-capacity AMs, but also the dissolving issue of lithium polysulfides in S-cathode.^[180]

3.3. Binder Engineering for ETN Control

The above strategies including core-shell design of AMs and flexible wrapping actually follow the same methodology: rational design of the structures of AMs incorporating nanostructured conductive agents. In parallel to these strategies, the efforts on polymer binders can also make a big difference in the ETN structures. It is well known that binders play a critical role in controlling the microstructures of the final electrodes and interactions among different components. Therefore, in this sub-section, we will summarize the main efforts on binder materials in order to build robust ETN structures in composite electrodes. These will include conductive binders, structural binders and self-healing binders.

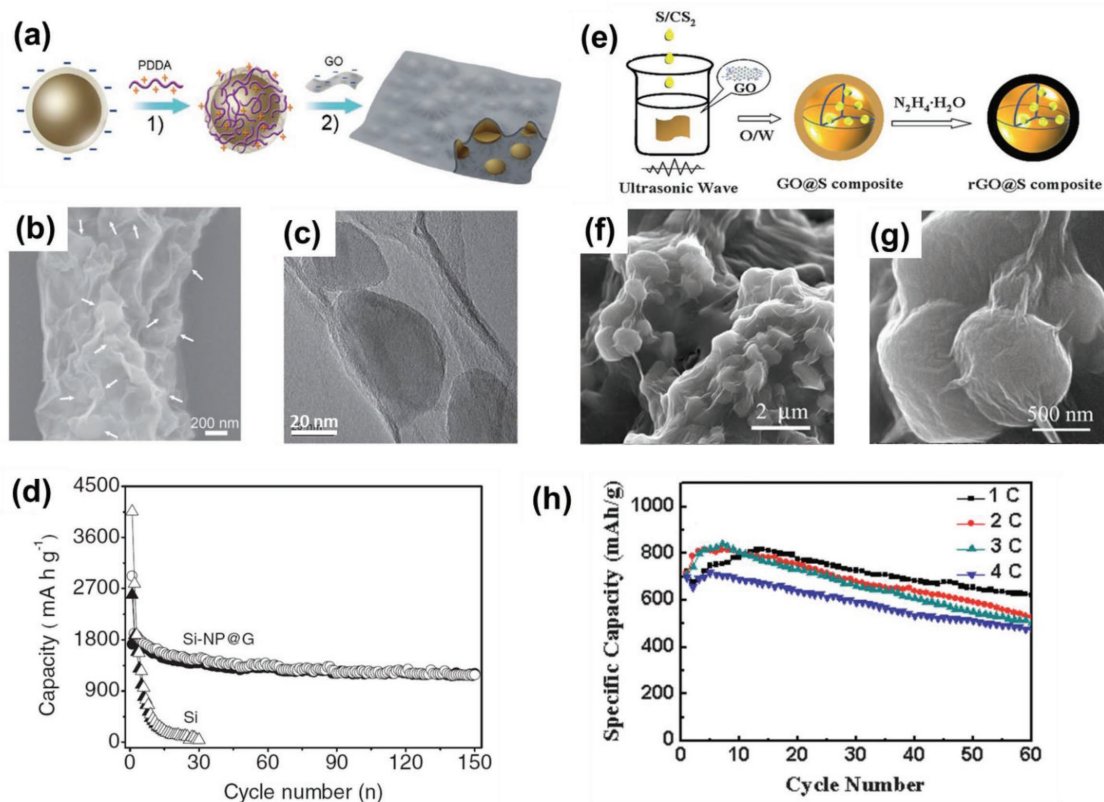


Figure 11. Flexible conductive wrapping for stabilizing ETN in high-capacity composite electrodes. a–d) Graphene-wrapped Si-NPs: a) Schematic of the fabrication strategy based on PDPA-assisted coating method. b,c), SEM and TEM images of the graphene-wrapped Si-NPs. d) cycle stability testing of the graphene wrapped Si-NPs. e–h) Reduced graphene oxide (RGO)-wrapped sulfur cathode: e) Schematic of the fabrication strategy based on sonication of sulfur solution in the presence of GO. f,g) SEM images the RGO-wrapped sulfur-NPs. h) cycle stability testing of the RGO@sulfur with different C-rates. a–d) Reproduced with permission.^[161] Copyright 2012, Wiley-VCH. e–h) Reproduced with permission.^[162] Copyright 2012, The Royal Society of Chemistry.

Conductive Binders: Similar to the conductive polymer coating in the core-shell strategy, conductive polymers are usually employed as functional binder to construct ETN in the composite electrodes.^[181–191] In this case, the conductive polymers act as both conductive agent and binder. For the construction of ETN, there are several significant advantages for polymeric conductive agent as compared with traditional carbon agent. First, polymeric conductive agent can give rise to more continuous pathway or conductive network, which is very different from carbon-based conductive agent that forms the conductive network by particle connection. Second, conductive polymers can form more uniform and strong interface with AM particles through a molecular coating process. Lastly, due to the above two advantages, the ETN built by conductive polymers is usually much stronger and stable than the ETN built by carbon-based conductive fillers. For example, Marschilok and co-workers reported a 3D nanostructured conductive gel framework based on PPy conductive polymer for Fe₃O₄ nanoparticles electrode as shown in **Figure 12a**.^[181] The PPy conductive binder formed uniform coating onto the Fe₃O₄ NPs and smooth connection among AM particles as shown by the SEM (see **Figure 12b**) and TEM images (see **Figure 12c**). At the same time, the PPy conductive binder was swelled by the liquid electrolyte and formed gel-type dual-conductive frame inside the composite electrodes. As a result, the cell resistance

was reduced from ≈ 50 to $\approx 30 \Omega$ (see **Figure 12d**) and the C-rate performance was notably improved (**Figure 12e**). Synthesis of new conductive polymers as functional binder is also of great interest. Different types of new conductive polymers have been developed by Liu's group.^[182,185,187,188] For instance, they chemically modified the conventional conductive polymer poly(1-pyrenemethyl methacrylate) (PPy) by a poly(1-pyrenemethyl methacrylate-co-triethylene oxide methyl ether methacrylate) (PPyE), in order to improve the adhesion of conductive polymer to Si-NPs (see **Figure 12f**). The SEM and TEM images as shown by **Figure 12g,h** confirmed the good adhesion of the conductive binder with Si-NPs. The improved adhesion between the PPyE and Si-NP significantly enhance the electrochemical performance and its stability as shown in **Figure 12i,j**. In particular, the C-rate performance at high current density, such as 1 C and 2 C, was improved notably. While, the cycle stability was dramatically improved, and a high specific capacity of $\approx 1500 \text{ mAh g}^{-1}$ @ 2C was achieved for the PPyE-Si electrode even after ≈ 1000 cycles. The much improved electrochemical performance is fundamentally contributed by the strong ENT based on the PPyE conductive polymer binder.

Structural Binders: The formation of ETN inside composite electrodes cannot happen without the help of binders and binders always play a critical role in controlling the structures of the ETN in composite electrodes.^[195] Structural binders do not have

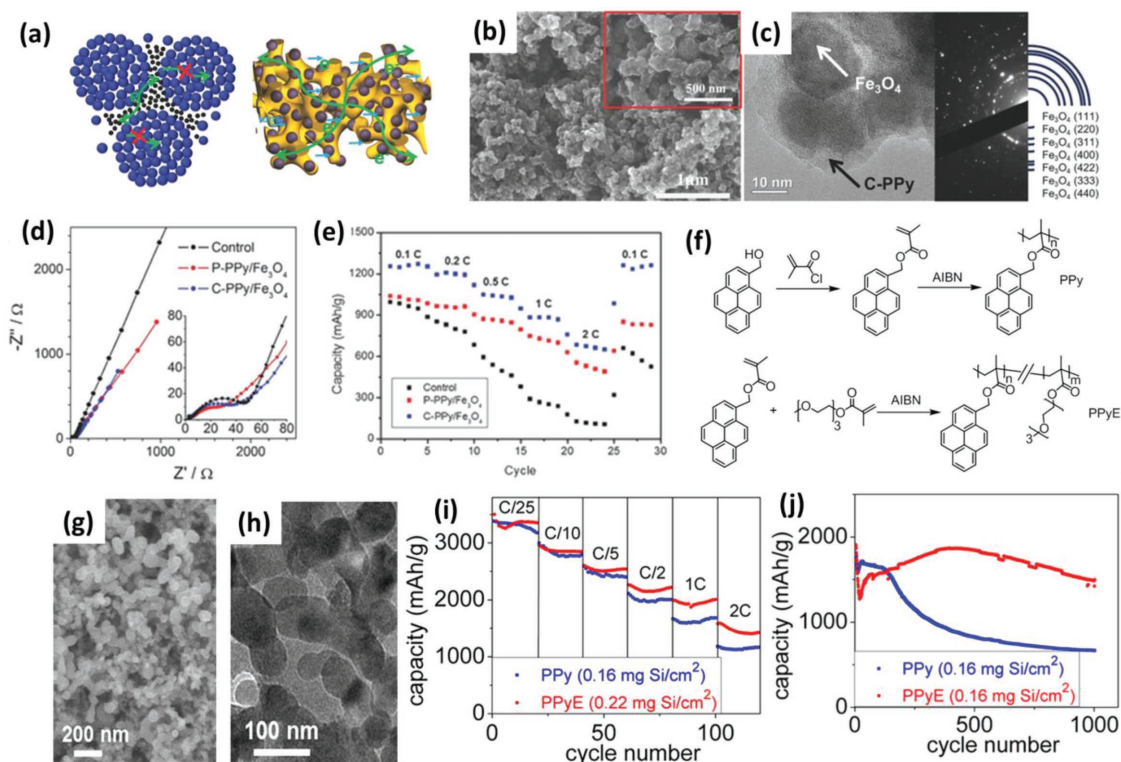


Figure 12. Conductive binders for ETN control in composite electrodes. a–e) 3D nanostructured conductive binder based on polypyrrole gel framework for Fe_3O_4 electrode: a) Schematic of the contribution of conductive binder to both electrons and ions transportation, b,c) SEM and TEM images of the resultant electrode composite, respectively. d,e) Nyquist curves and C-rate performance of the cells, respectively. f–j) Polymer binder with conductive side chain (PPyE) for stabilizing ETN in Si anode: f) Scheme of the synthesis process of the PPyE. g,h) SEM and TEM images of the Si anode composite based on the conductive polymer binder. i,j) C-rate performance (i) and cycle stability (j) of the PPyE–Si anode. a–e) Reproduced with permission.^[181] Copyright 2017, Wiley-VCH. f–j) Reproduced with permission.^[182] Copyright 2015, American Chemical Society.

conduction function, but they are able to improve or reinforce the structures of the ETN that uses conductive fillers as the building block. Compared with traditional PVDF binder, structural binders usually show much improved adhesion properties with both conductive agents and/or AMs particles, better mechanical properties (such as flexibility) and other possible properties.^[192–194,196] Clearly, conductive nanofillers (e.g., carbon black, carbon nanotubes, nanofibers, etc.) are still the most primary building block for the construction of ETN inside composite electrodes. Therefore, studies on new structural binders with ability to improve the structures and properties of the ETN are still in critical need by the mass-production of advanced electrodes, such as the electrodes with high-capacity AMs. There are several ways to the design of structural binders: polymer alloying, chemical bonding with AMs, and self-healing polymers rich in H-bonds.

The first one, also the simplest one, is the physical method by molecular blending or alloying.^[192,197,198] For example, Wang and Zhong and co-workers reported a type of polymer alloy binder to control the structures-properties of battery electrodes as shown in Figure 13a.^[192] Based on the most classic polymer binder, PVDF, they modified PVDF binder by ultrahigh molecular weight poly(ethylene oxide) (UHMWPEO) simply via polymer alloying, which has been well known in polymer science and widely employed to improve the mechanical properties of polymeric materials. They found that the mixing of PVDF with UHMWPEO can significantly suppress the crystallization

of each component and improve the adhesion and mechanical flexibility of the binder. As a result, a flexible electrode composite with much improved dispersion/distribution uniformity for the conductive agent and notably improved mechanical flexibility was fabricated as shown by Figure 13b–e. The improved adhesion of the alloy binder and uniformity of the conductive agent are mainly contributed by the amorphous structures of the alloy binder. Another study on advanced structural binders by polymer blending was reported by Zhang and co-workers who developed a type of biopolymer network binder for the stabilization of ETN and blocking of polysulfides in high-performance Li–S batteries.^[198] The second method is to chemically modify binder polymers in order to achieve much improved adhesion properties with AMs or mechanical strength. For example, as shown in Figure 13f, Coskun and co-workers reported a hyper-branched β -cyclodextrin polymer as advanced structure binder for Si-anode.^[193] This polymer can generate strong hydrogen-bonding interaction with Si-anode and so improve the stability of ETN during the big volume change of Si-anode after different cycles (see Figure 13g,h). Another good example is the mussel-inspired adhesive binder reported by Park and co-workers.^[194] As shown in Figure 13i, they got inspiration from mussel that realizes strong bonding between muscle and inorganic shell, and designed a type of adhesive binder named as Alg-C. With the help of this binder, Si-anode showed notably improved structure integrated and adhesion with the copper substrate as shown by the peeling testing in

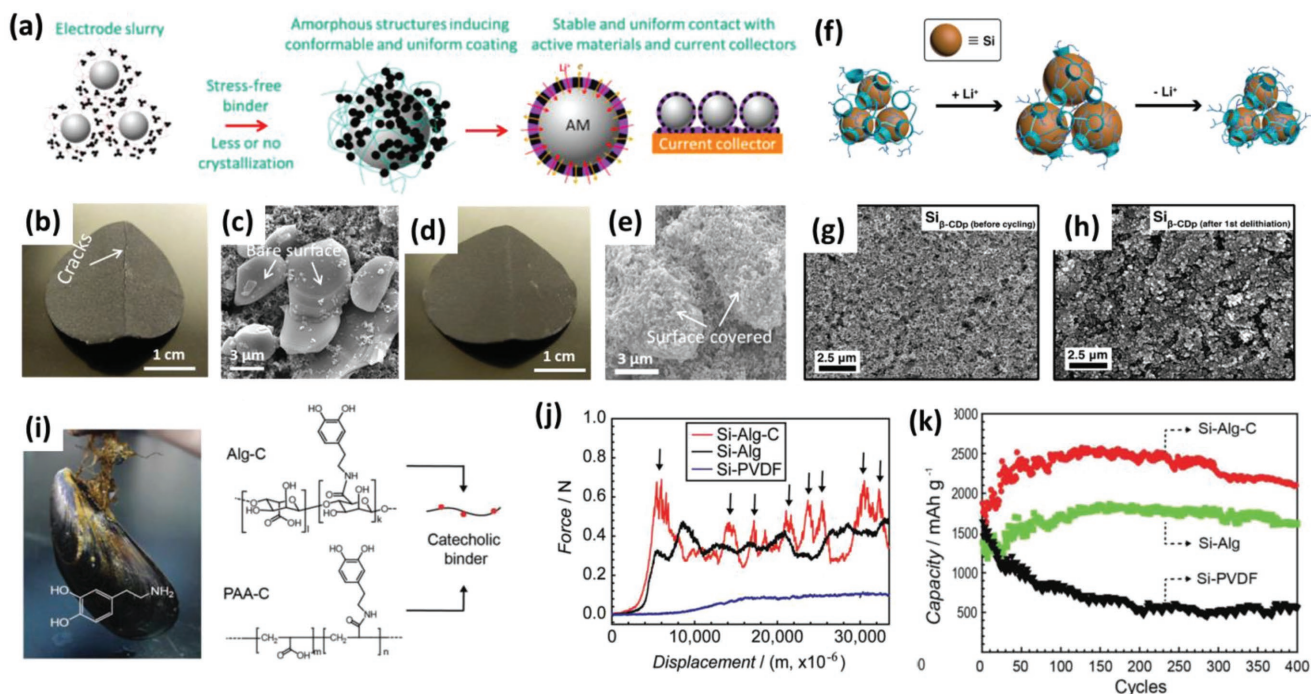


Figure 13. Structural binders for ETN reinforcement. a–e) Polymer alloy binder for adjusting the structures of ETN in electrode composite: a) Schematic of the structural evolution of composite electrodes using stress-free polymer alloy as advanced binders. b) Digital photo showing brittle behavior of electrode composite using traditional PVDF binder. c) SEM image of electrode composite with PVDF as the binder. d) Digital photo showing flexible behavior of electrode composite using PVDF-UHMWPEO alloy binder. e) SEM image of electrode composite with PVDF-UHMWPEO alloy binder. f–h) Structural binder enabling hydrogen-bonding interaction with Si-anode for stabilizing the ETN: f) Schematic of the stabilization mechanism. g, h) SEM images of the Si-anode composite before cycling and after first delithiation, respectively. i–k) Mussel-inspired structural binder for Si-anode: i) The structure formula for a mussel-inspired adhesive binder Alg-C. j) Peeling testing for the Si-NP anode with different types of binders. k) Cycling stability of the resultant Alg-C/Si-NP electrode at 0.5 C. a–e) Reproduced with permission.^[192] Copyright 2018, Elsevier. f–h) Reproduced with permission.^[193] Copyright 2014, American Chemical Society. i–k) Reproduced with permission.^[194] Copyright 2013, Wiley-VCH.

Figure 13j). As a result, Si-anode with this strong adhesive binder showed very good cycle stability as shown in Figure 13k. Lastly, repairing the broken ETN by self-healing chemistry represents another attractive strategy for developing structural binder that can realize robust ETN in composite electrodes. This strategy was initially proposed by Cui and co-workers, and it is attracting notable attention for the studies on Si-anode.^[199–203] The self-healing polymers usually have multiple intermolecular or intramolecular H-bonding sites which can repair the cracks induced by the volume change of AMs. These studies indicate that strong adhesion, good mechanical properties or even self-healing properties are critical factors of structural binders for building robust ETN and stabilize the electrochemical performance.

Since binder works together with conductive agents as the building blocks for the ETN, the types of conductive agents also fundamentally affect the structures and properties of the ETN, and thus impact the electrochemical performance.^[6,204–207] For example, 0D, 1D, and 2D carbon materials can generate an ETN with different 3D structures, mechanical properties and stability with strain. One can even build binder-free ETN with 1D or 2D carbon materials.^[208–210] At the same time, 1D or 2D carbon is beneficial to the network connectivity of ETN, which improves the conductivity and its stability with strain. This is critical for achieving good cycle stability and C-rate capability for especially high-capacity AMs.^[211–215] However, 0D conductive carbon is

beneficial to uniform electronic contact with AM. In short, a rational design of binder/conductive composites is still a facile and effective strategy for ETN control. However, more efforts should be focused on improving the distribution uniformity, mechanical strength or flexibility and adhesion properties with AMs.

4. Controlling Both ETN and ITN in Composite Electrodes

In the above sections, we have introduced some strategies based on their main contribution to either ETN or ITN. In fact, since ETN and ITN are usually entangled and coupled inside composite electrodes, it is hard to clearly separate them from each other. Therefore, there are many strategies that can control the ETN and ITN simultaneously. These strategies include electrode templates, electrode scaffolds, electrode matrices, etc., which will be introduced below.

4.1. Electrode Templates

Template methods have also been widely employed to control both the ITN and ETN in electrodes. Sacrificing templates based on colloid crystals is the most popular way to constructing

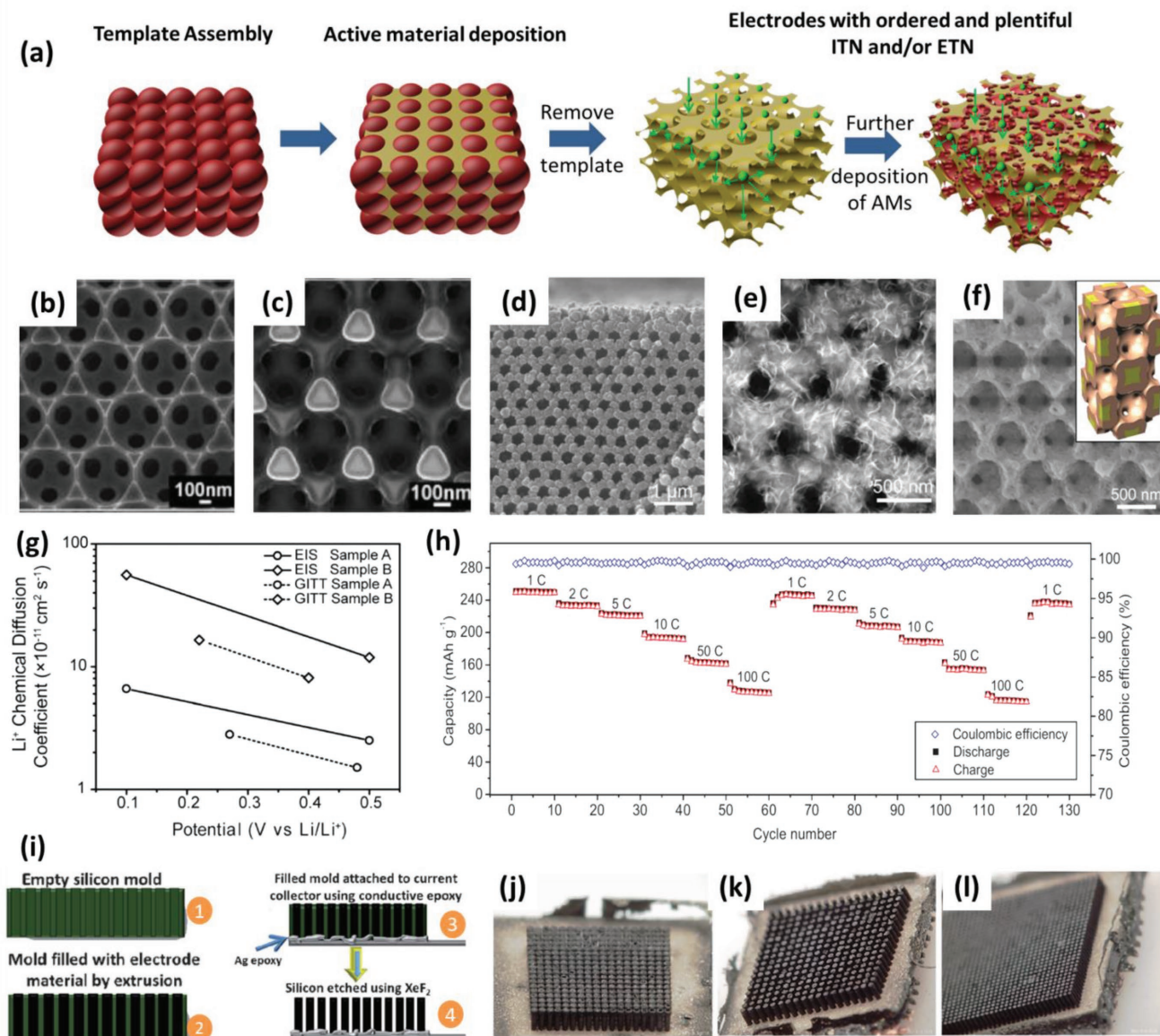


Figure 14. Electrode template strategy for building ordered ITN/ETN in composite electrodes. a) Illustration of the template strategy based on colloid crystals to build ordered pores for fast ions-transport. b,c,g) Si electrode with ordered porous structures by Ni inverse opal template method: b) SEM image the Ni inverse opal after template removal (plane view). c) SEM image of the structure after Si deposition by CVD (plane view). g) Li^+ -diffusion coefficient in templated Si-anode with different pore size. d,e) Combination of Ni inverse opal template with hydrothermal deposition for fabrication of multi-layered inverse opal template electrodes: SEM images of $\text{SiO}_2/\text{Fe}_3\text{O}_4$ and $\text{Ni}@\text{SnO}_2\text{-NPs}@\text{SiO}_2$ inverse opal electrodes, respectively. f,h) 3D sandwich-structured electrode with controlled pores based on inverse opal template: f) Cross-sectional-view SEM image of a $\text{V}_2\text{O}_5@\text{graphene}@\text{V}_2\text{O}_5$ sandwich-structured electrode. h) C-rate performance of the $\text{V}_2\text{O}_5@\text{graphene}@\text{V}_2\text{O}_5$ sandwich-structured electrode. i–l) 3D electrode with ordered structures based on a silicon template: i) Illustration of the fabrication process. j–l) The fabricated three-dimensional carbon array electrodes with aspect ratio of 5.5:1, 3.5:1, and 7:1, respectively. b,c,g) Reproduced with permission.^[216] Copyright 2012, American Chemical Society. d,e) Reproduced with permission.^[217] Copyright 2014, Wiley-VCH. f,h) Reproduced with permission.^[219] Copyright 2016, Wiley-VCH. i–l) Reproduced with permission.^[223] Copyright 2014, Wiley-VCH.

well-defined ITN and ETN structures. As illustrated in **Figure 14a**, the colloid crystal is first built onto a substrate, usually the current collector. Then active materials or conductive agent are deposited onto the 3D-ordered template. After the removal of the template, an electrode or 3D conductive scaffold with template-defined porous structures can be achieved. Based on this porous scaffold, one can deposit additional active materials. This template method has been comprehensively studied

mainly by Braun's group.^[216–222] **Figure 14** shows some of the examples. For instance, as shown in **Figure 14b**, a 3D nickel metal scaffold was first prepared via a colloidal crystal template method. Then, a 3D bi-continuous silicon anode was fabricated by depositing a layer of silicon on the surface of the 3D nickel metal scaffold as shown in **Figure 14c**.^[216] This method is very attractive as it realizes a well control of both ETN (i.e., the metal scaffold) and ITN (i.e., the porous structures) via one template.

Based on this strategy, 3D nanostructured electrodes with more complicated compositions can be realized. For example, Braun and co-workers further developed a type of 3D $\text{SiO}_2@\text{Fe}_3\text{O}_4$ (see Figure 14d) and 3D $\text{Ni}@\text{SnO}_2\text{-NPs}@\text{SiO}_2$ inverse opal electrodes (see Figure 14e),^[217] and even $\text{V}_2\text{O}_5@\text{graphene}@\text{V}_2\text{O}_5$ sandwich-structured composite electrode (see Figure 14f).^[219]

The well-controlled pore structures by electrode template method provide fast channels for Li-diffusion inside the electrode. For example, pores with bigger size definitely help the fast diffusion of Li-ions as shown in Figure 14g. Benefited from the well-defined ETN and ITN structures, one can significantly improve the transport efficiency for both ions and electrons and enable ultrafast charge and discharge capability (see Figure 14h).^[219,222] At the same time, the well-defined pore structures also provide space for the volume change of active materials (see Figure 14b,c). In addition to colloid crystals, there are many other types of electrode templates that can generate well-controlled 3D structures for electrodes. For example, Dunn and co-workers reported a silicon template method for fabrication of 3D carbon array electrodes with different aspect ratios and pore configuration.^[223] As shown in Figure 14i, the authors employed empty silicon mold as the electrode template and the AMs was filled into the empty space by extrusion. After removal of the silicon mold, electrodes with well-defined array structures can be fabricated. They have successfully fabricated several array electrodes with different aspect ratios and pore configuration as shown in Figure 14j–l. For a more comprehensive summary on 3D structured electrodes with well-defined ITN and ETN, it is suggested to read the reviews by Dunn,^[224–226] Rolison, Long, and Gogotsi et al.^[226,227]

4.2. Electrode Scaffolds/Frames

Different from the strategy of electrode templates that is removed finally, electrode scaffolds/frames stay inside the

electrode as a component providing physical support for holding the active materials and shaping the ITN/ETN inside the final composite electrodes. They are usually porous conductive sheets with good mechanical properties. There are several types of electrode scaffolds made of different materials or prepared via different methods, for example, metal foams, graphene-based foams, carbon-based fabrics/frameworks, etc., which will be introduced below.

Metal Foams as Highly Conductive and Mechanically Strong Electrode Scaffolds: Metal foams have been frequently studied as a type of electrode scaffold for different types of electrochemical devices, including lithium ion batteries,^[228–233] lithium-sulfur batteries,^[234] supercapacitors, etc.^[235–239] The high conductivity, high porosity and mechanical strength make metal foams an idea candidate for electrode scaffold. At the same time, it is easy to load nanostructured AMs onto the metal scaffolds, such as, by electrochemical deposition^[240–243] or chemical vapor deposition.^[240,244,245] The most popular metal foams studied in this area include nickel foam and copper foam.^[246–251] For example, as shown in Figure 15, Hng and co-workers reported a design of 3D ordered hierarchically porous Fe_2O_3 electrode based on nickel foam.^[228] As illustrated in Figure 15a, they first deposited a colloid template onto the Ni-foam, and then the template was removed and the active material, Fe_2O_3 nanoparticles, was formed by in-situ crystallization from its precursors of Fe^{3+} . Simultaneously, glucose in the precursor solution was employed as carbon source, which was carbonized into ordered 3D macroporous carbon that firmly integrated on the framework of Ni foam as shown by Figure 15b. This unique hierarchically porous $\text{Fe}_2\text{O}_3@\text{C}$ electrode obviously possesses a robust ETN constructed by the Ni-foam and the 3D macroporous carbon coated on the Ni-foam, and a robust ITN with pore size larger than $300\ \mu\text{m}$ that is defined by the highly porous structure of the Ni-foam. Benefited from these powerful transport networks, the electrode showed an ultrahigh rate capabilities and delivered

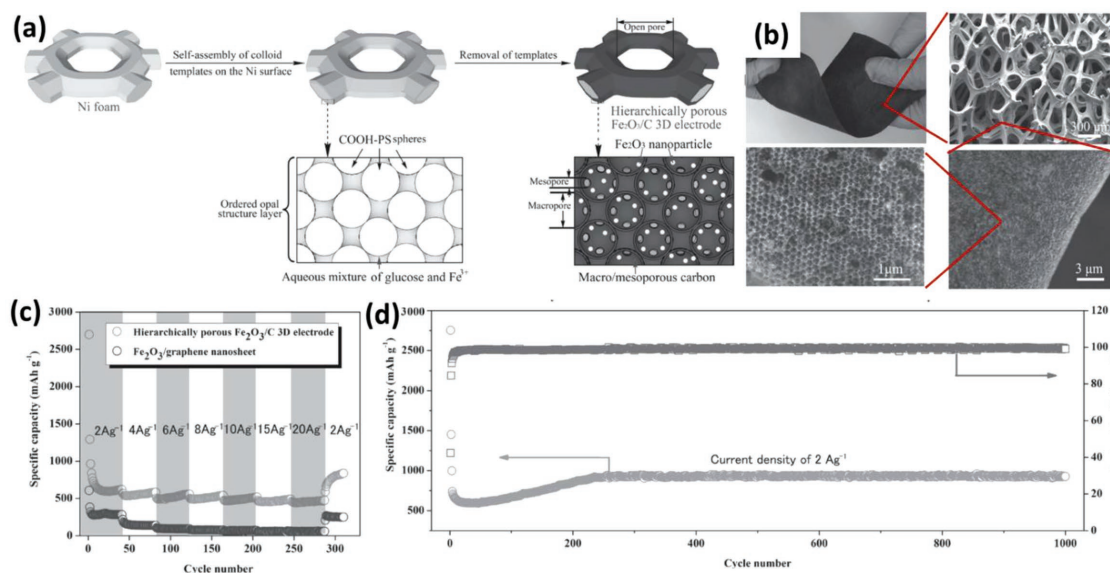


Figure 15. Metal-foam-based electrode scaffolds. Nickel foam as electrode scaffold for growing porous Fe_2O_3 active materials with building robust ETN and ITN: a) Scheme of the fabrication process combining self-assembly of colloid template and Ni-foam. b) Digital photo and SEM images of the Ni-foam supported composite electrodes. c, d) C-rate and cycle performance. Reproduced with permission.^[228] Copyright 2014, Wiley-VCH.

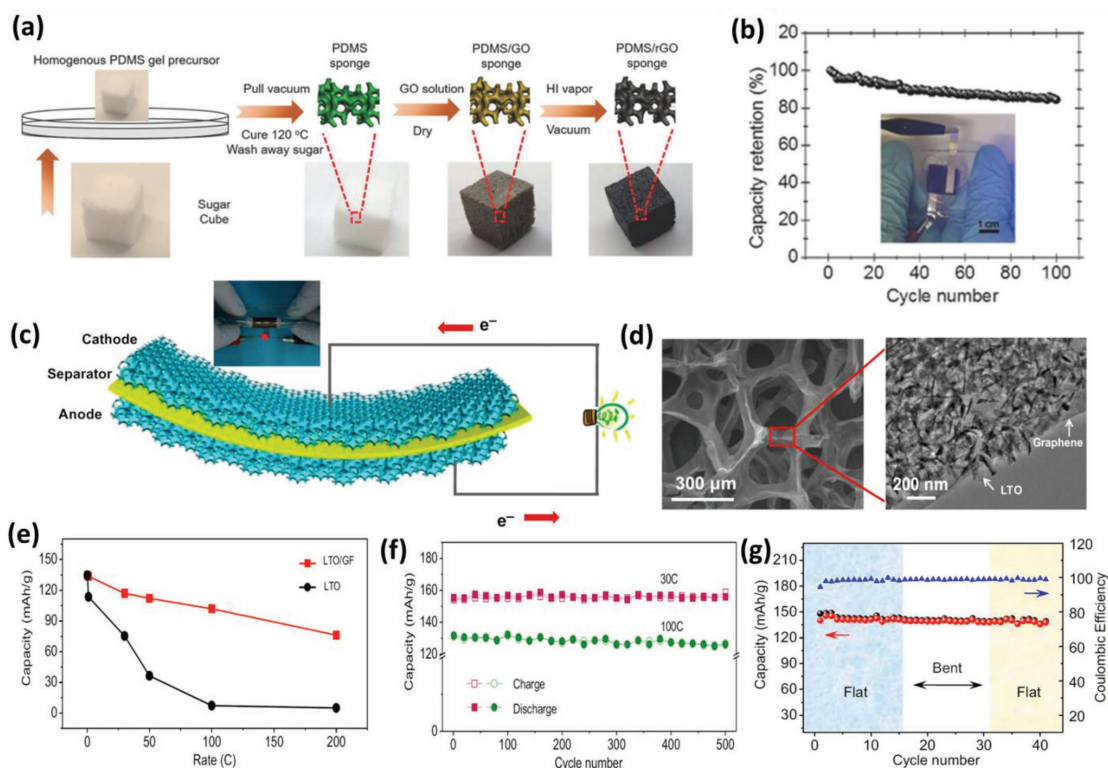


Figure 16. Graphene foam as flexible electrode scaffold. a,b) Stretchable electrode frame based on PDMS/rGO sponge: a) Schematic of the fabrication process, b) cycle stability of a stretchable PDMS/rGO sponge/VOPO₄//PDMS/rGO sponge/hard-carbon sodium-ion full battery. c–g) 3D interconnected graphene foam (GF) as flexible electrode frame: c) Illustration of the structures of a flexible full cell based on the GF electrode frame. d) SEM and TEM images of composite electrodes with robust ETN and ITN (porous structures). e,f), C-rate and cycle performance for an LTO–GF anode, respectively. g) Electrochemical performance of a flexible LTO/GF//LFP/GF full battery under bent and flat states. a,b) Reproduced with permission.^[261] Copyright 2017, Wiley-VCH. c–g) Reproduced with permission.^[262] Copyright 2012, National Academy of Sciences.

a high specific capacity of $\approx 500 \text{ mAh g}^{-1}$ even at 20 A g^{-1} (see Figure 15c). At the same time, they demonstrated excellent cycle stability at a high current density of 2 A g^{-1} . In particular, the specific capacity ($\approx 900 \text{ mAh g}^{-1}$) showed even no decay even after 1000 cycles as shown by Figure 15d, indicating that there was a very stable charges transport system in the electrode.

Graphene-Based Foam as Electrode Scaffold: Due to the excellent conductivity, ultrahigh surface area, good mechanical flexibility, and electrochemical performance, graphene is a very promising nanomaterial for building advanced conductive networks in ESDs. Actually, it has been widely used as an advanced conductive agent to replace the conventional ones, such as carbon black,^[252–256] or directly used as anode active materials.^[257–260] Therefore, graphene-based foams are also of great interest for ESDs to achieve ultrahigh rate capability and even mechanical flexibility.^[261–267] Graphene-based foams may have some significant advantages as compared with metal foams, such as much lower density, excellent electrochemical stability, flexibility in fabrication, etc.

For example, Yu and co-workers proposed a sugar-template method to prepare elastic graphene foam (GF) based on PDMS sponge as illustrated in Figure 16a.^[261] They first prepared a PDMS/sugar composite which was cured first and then etched by water to achieve an elastic PDMS sponge. Based on this sponge, GO was coated and reduced into rGO by HI vapor.

Finally, they loaded AMs (VOPO₄ as cathode and hard carbon as anode) into the PDMS/rGO foam to fabricate a full sodium ion battery showing excellent flexibility and even stretchability. The electrochemical performance as shown in Figure 16a indicates that the flexible PDMS/rGO foam can support stable charges transport for more than 100 cycles even under stretching. Another example on using graphene foam as flexible electrode scaffolds was reported by Cheng and co-workers.^[262] In this study, the authors fabricated a unique 3D GF consisting of a 3D interconnected network structure by high-quality chemical vapor deposition method. The electrical conductivity of this high-quality GF was estimated as high as $\approx 1000 \text{ S m}^{-1}$. Moreover, the reported GF is extremely light with an areal density of only about 0.1 mg cm^{-2} , and a high porosity of $\approx 99.7\%$. As illustrated in Figure 16c,d, they further demonstrated a thin, lightweight, and flexible full cell with LFP/GF and LTO/GF as the two electrodes. Benefited from the GF scaffold, they were able to achieve a high specific capacity of $\approx 90 \text{ mAh g}^{-1}$ even with a current density of 200 C (see Figure 16e) for LTO anode. At the same time, the full cell based on the GF showed very high charge and discharge rates up to 100 C (see Figure 16f). More significantly, the full cell is very flexible and was capable of repeated bending to a radius of $<5 \text{ mm}$ without breaking the charges-transport networks and loss of performance as shown in Figure 16g.

Carbon-Based Electrode Scaffolds/Frames: The metal foams and graphene foams as introduced above usually possess very big pores (around 300 μm), which is beneficial to build robust ITN, but sacrifices too much space and so energy density. In addition, the mechanical properties of these foams (such as compression modulus) are very critical for the final porous structures of the electrodes under compression since foams are highly compressible due to the high porosity and flexibility. Therefore, strategies on how to design the porous structures of electrode scaffolds to improve the mechanical properties and support higher loading of AMs are in critical need. Carbon foams and porous carbon frameworks with small pores provide a good solution to the above issue.^[268–274] For example, Zhang and co-workers reported a type of porous carbon foam based on CMK-3 hard template for LTO anode as shown in Figure 17a.^[268] They first prepared the CMK-3 foam template by the replication of mesoporous

silica SBA-15.^[275] The CMK-3 foam was further treated by concentrated nitric acid to induce good affinity for facile impregnation of the precursor aqueous solution of AMs (LTO). Finally, the well-dispersed LTO nanoparticles formed inside the CMK-3 foam after a heat treatment at 750 $^{\circ}\text{C}$. This strategy provides a good control on the porous structures of the carbon foam and so advanced ETN and ITN structures as illustrated by Figure 17b. Figure 17c is a TEM image of the LTO/CMK-3 foam composite which shows uniform distribution and dispersion of LTO NPs inside the carbon foam. When employed as an anode material for LIBs, it exhibited greatly improved electrochemical performance as compared with bulk LTO. In particular, it did not only show an excellent rate capability (73.4 mAh g^{-1} at a high current density of 80 C (see Figure 17d), but also significantly enhanced cycling stability with only 5.6% capacity loss after 1000 cycles at a high rate of 20 C (see Figure 17e).

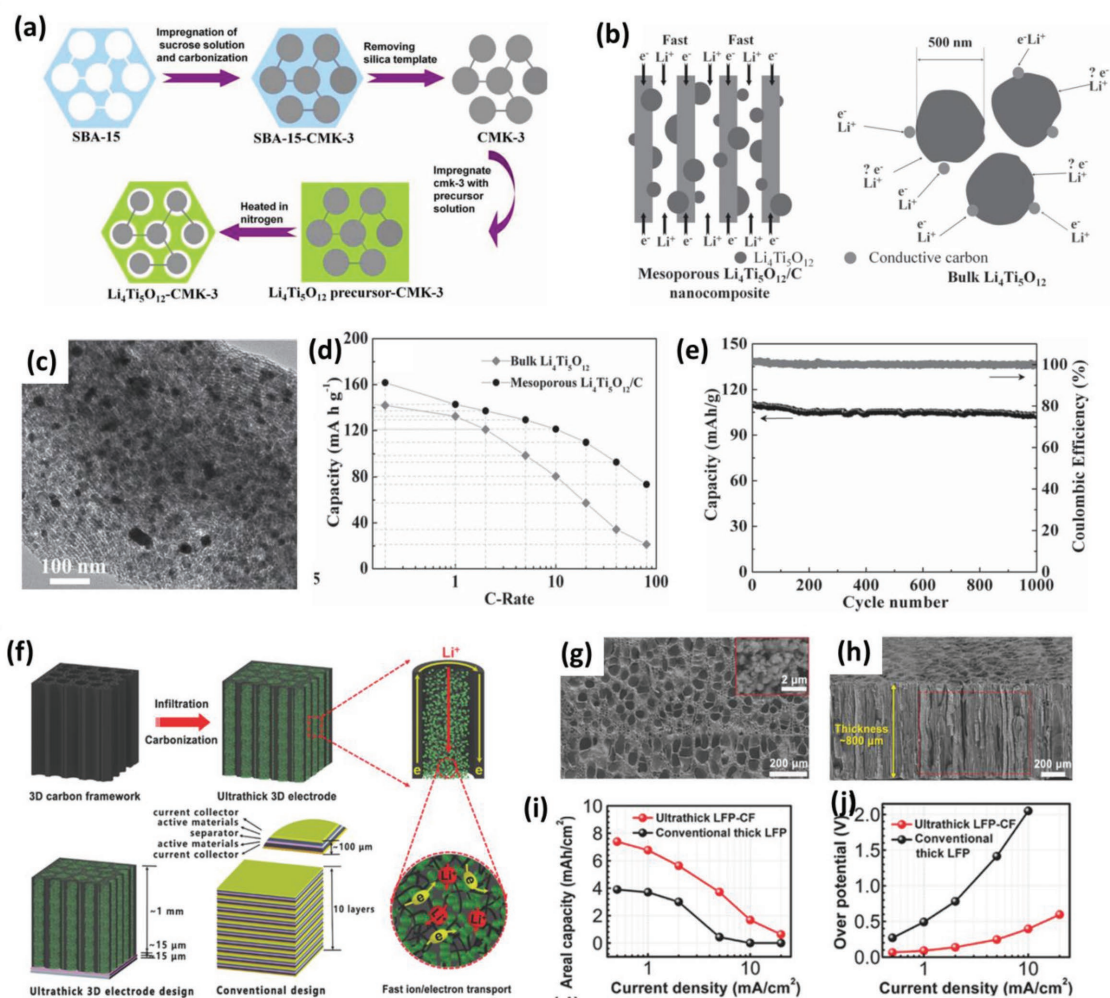


Figure 17. Carbon foam and bio-derived carbon framework as advanced electrode scaffolds enabling fast charges transport. a) Schematic of the fabrication of $\text{Li}_4\text{Ti}_5\text{O}_{12}/\text{C}$ nanocomposite based on ordered mesoporous CMK-3 carbon foam. b) Illustration of the contribution to fast ions and electrons transportation from the ordered carbon foam. c) TEM image showing the microstructures of $\text{Li}_4\text{Ti}_5\text{O}_{12}/\text{C}$ nanocomposite. d, e) C-rate and cycle performance of the $\text{Li}_4\text{Ti}_5\text{O}_{12}/\text{C}$ nanocomposite electrode, respectively. f) Bio-derived electrode scaffold for fabrication of thick electrodes with low-tortuosity for both electrons and ions transport. g, h) SEM images of a thick electrode composite with ordered channels for both ions and electrons transport. i, j) areal capacity and overpotential at different current densities for the thick electrodes based on the carbon template. a–e) Reproduced with permission.^[268] Copyright 2012, Wiley-VCH. f–j) Reproduced with permission.^[269] Copyright 2017, Wiley-VCH.

Nature materials with well-defined microstructures, such as woods, animal shells, provide another important source for fabrication of porous carbon which can potentially be modified as advanced electrode scaffolds.^[269,270,276–288] These bioderived porous carbon materials are very attractive for application in ESDs it is not only because the raw materials are more sustainable and environmentally friendly, but also their porous structures are very unique (e.g., very uniform pore size and even well-aligned pore configuration). For example, as illustrated in Figure 17f, Hu and Xie and co-workers reported a study on fabrication of thick electrode based on an advanced carbon framework with aligned pores that were derived from natural wood materials.^[269] This unique carbon framework is highly conductive, lightweight, and importantly, naturally designed with low-tortuosity. When employed as an electrode scaffold, they demonstrated an ultrathick 3D electrode with lithium iron phosphate as the AMs (see Figure 17g,h). The thickness of the electrode is about 800 μm and the active material mass loading reached as high as 60 mg cm^{-2} . With such a high loading level of AM and thickness, the battery still delivered a high areal capacity of 7.6 mAh cm^{-2} @ 0.1 mA cm^{-2} and $\approx 2 \text{mAh cm}^{-2}$ @ 10 mA cm^{-2} (see Figure 17i). Moreover, the over-potential of the cell was significantly reduced by the unique carbon framework as compared with conventional thick electrode as shown in Figure 17j, indicating a powerful charges (both ions and electrons) transport inside the thick electrodes. Other natural materials, such as crab shell,^[276] were also studied as electrode scaffold by Cui, Cheng, Wong et al.

As introduced above, electrode scaffolds/frames provide a facile way to simultaneously control of the ETN and ITN. The roles of electrode scaffolds/frames can be understood by the following three points. First, for ETN, they provide a robust conductive skeleton with superior structural stability, mechanical properties, and conductive properties as compared with traditional ETN built by binder/conductive agent composites. Second, due to the unique porous structures, they expand and shape the ITN in a way of facilitating fast ion transport. Third, the interfaces between ETN and AM can be improved if the AM is deposited or grown on the ETN surface. All these advantages together give rise to the much superior electrochemical performance as introduced above. However, it is noted that there is still a long way to go for their practical applications. For example, the demonstration of the high specific capacity and C-rate capability is realized by notably sacrificing the overall energy density since the ETN and ITN occupy too much space or weight inside the electrode. Moreover, one can expect a significant increase in material and manufacturing cost if electrode scaffolds/frames are finally used in the ESDs. In spite of these facts, from scientific point of view, they provide strong evidence on how important a robust charge transport system is for the electrochemical performance.

4.3. Electrode Matrix

The above strategies are designed for porous electrodes that have to work with liquid electrolytes in the final ESDs. With the development of ESDs, design of advanced nonporous electrodes that integrate all the functions (ion-conduction, electron-conduction, and ion-storage) in one composite is important for

the development of advanced ESDs. With the help of nonporous electrode composite design, one can potentially solve the challenging issues for porous electrodes, including interface weakness, structural/mechanical instability, and poor controllability over the microstructures of ETN and ITN and also safety concern. The realization of this design is fundamentally dependent on the development of advanced solid or gel electrolytes. With the increasing interests on all-solid-state ESDs, it is believed that strategies on and design and fabrication of nonporous composite electrodes with solid electrolytes will become more and more critical. As an attempt to realize this goal, the authors proposed the concept of electrode matrix which was learned from the matrix well-known in polymer nanocomposites.^[289] As illustrated in Figure 18a, we fabricated a gum-like nanocomposite as a unique electrode matrix to integrate the essential properties/functions in one material: ion-conductivity, electron-conductivity, adhesion, mechanical properties, and even processing properties. Based on this gum-like electrode matrix, one can fabricate nonporous composite electrodes with in-built uniform ETN and ITN around the AMs as illustrated in Figure 18b. Via a rational design of the compositions for the gum-like nanocomposite, good processability by such as extrusion was also realized as demonstrated in Figure 18c.

Based on this electrode matrix, we successfully demonstrated a nonporous electrode composite with 70 wt% loading of LiCoO_2 and 30 wt% loading of the electrode matrix as shown in Figure 18d. Significantly, the nonporous electrode composite showed excellent mechanical flexibility due to the good interfaces among different components. Figure 18e,f shows the SEM images of the fracture and free surface of the nonporous composite electrodes. From these images, one can find that the gum-like electrode matrix can form very uniform and strong interfaces with AM particles, which explains the good mechanical flexibility. As a proof-of-concept study, we further investigated the electrochemical performance in a half-cell with lithium metal as the anode. As shown in Figure 18g, the battery with the electrode matrix gave rise to a similar specific capacity (130 mAh g^{-1} @ 0.5C) as compared with traditional porous LCO electrode. However, the cycle stability of the half-cell is more stable than the porous counterpart. This result also indicates that the nonporous composite electrodes and gum-like electrolytes^[290,291] may also improve the surface stability of lithium metal.

An electrode matrix, as a new concept learned from polymer composites, integrates the functions of the binder, electrolyte and conductive agent into one material. This will significantly simplify the structures of electrode composites. At a unique polymeric nanocomposite, the structures and properties of the electrode matrix can be adjusted, or even, customized for a specific ESD to achieve the desired performance. With the increasing interest in semi-solid-state or all-solid-state batteries, the electrode matrix will play a more and more critical role in the future ESDs. However, there are also some issues. First, the performance and properties of an electrode matrix need improvement in several ways, such as, ionic conductivity and/or mechanical properties. This is highly dependent on the development of highly ion-conductive solid polymer electrolytes or gel polymer electrolytes. Second, the energy density of the nonporous composite electrode needs improvement. This issue may be resolved by using high capacity AMs, such as silicon

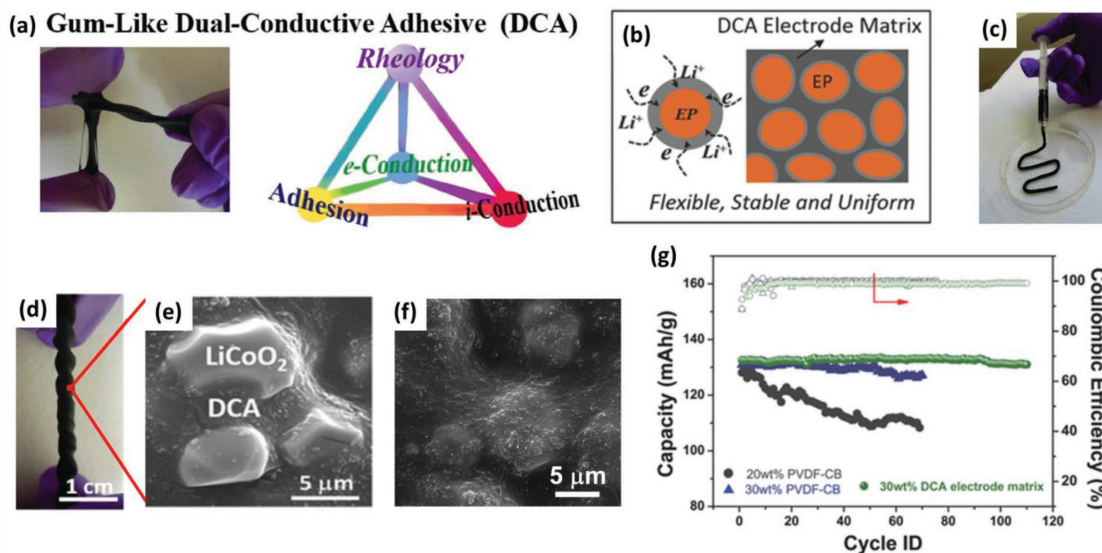


Figure 18. Electrode matrix integrating ion and electron conduction functions into one nonporous nanocomposite for the structure–property control of composite electrodes. a) Schematic of the concept of electrode matrix based on a gum-like dual-conductive adhesive that integrates all the critical properties in one material. b) Illustration of nonporous composite electrodes based on the gum-like electrode matrix. c) Digital photos showing the good processability of the gum-like electrode matrix by extrusion. d) Digital photo showing the mechanical flexibility of the resultant nonporous electrode composite under twisting. e, f) SEM images of the fracture and free surface of the nonporous composite electrodes with uniform and good interfaces. g) cycle stability testing of a nonporous LCO/Li half-cell with the gum-like electrode matrix. a–g) Reproduced with permission.^[289] Copyright 2016, Wiley-VCH.

and sulfur. In short, the development of electrode matrix is still at its early stage and the knowledge/technology to be well established for polymer nanocomposites will be very instructive.

5. Concluding Remarks

5.1. Summary

The charge transport networks, including ITN and ETN, are the veins inside composite electrodes. Their structures and properties have significant influence on the electrochemical performance, which is especially true for high capacity active materials (e.g., silicon, sulfur, nickel-rich and lithium-rich cathodes). In particular, nickel-rich and lithium-rich cathodes are of great interest for EV applications. In this case, building robust ETN and ITN to support fast charging/discharging becomes very critical. Moreover, in addition to the current focus on stabilizing lithium-rich cathode particles, how the structures/properties of ETN/ITN affect their performance is also a critical task for the R&D of Li-rich high-capacity AMs.^[292–295] Therefore, the strategies summarized above are instructive for all the different types of advanced batteries that need a powerful charge transport system. It should be noted that ITN and ETN are not a real component inside an energy storage device, but a production of the teamwork among all the components, the manufacturing process and even the electrochemical reactions. Therefore, the strategies for controlling the structures and properties of ITN/ETN vary from component design to electrode even cell design, from manufacturing to assembly, as summarized in this review.

For the ITN around AMs, the morphology/structure control of each component (e.g., porous active materials), electrode

design with sacrificing additives, additive manufacturing generating programmable pores, etc. are very effective methods for the control of the ITN structures. As summarized in **Table 1**, there are always advantages and disadvantages for each strategy. For example, the ion-transport capability can be notably improved by the strategies producing increased porosity (i.e., porous AMs, electrode additives) or decreased tortuosity of the porous structures. However, usually there is a sacrifice of volumetric energy density or an increasing of manufacturing cost finally. In addition, the increased porosity may weaken the mechanical properties of the whole composite electrode and thus, induce structural instabilities, which notably affect the performance stability. However, in this scenario, there is exception. For example, if one can achieve ordered ITN with optimal porosity, the trade-offs among volumetric energy density, power density, and even mechanical stability may be resolved. This has been demonstrated by the template additive strategy as reported by Chiang and co-workers.^[58] Therefore, the future efforts on ITN control can be concentrated on the optimization of ITN structures through materials or manufacturing engineering. The primary goal is to achieve rational structures (e.g., gradient and ordered structures) and volume fraction (porosity) to support fast ion-transport as well as high volumetric energy density. This is one of the keys for the development of electrical vehicles that rely on advanced batteries with both high energy and power densities.

For ETN, the structures and properties (mechanical and conductive properties) are usually not the primary limiting factors for traditional active materials. However, with the increasing interest on high-capacity active materials (e.g., Si, sulfur, etc.), they become very critical as introduced in this review. Here, we have introduced seven strategies to reinforcing ETN structures and properties as summarized in Table 1. The first group of

Table 1. Summary of the main strategies for controlling transport networks in electrodes.

Strategies	ITN control	ETN control	Advantages	Possible disadvantages	Ref.
Random close packing	NA	NA	Universal, low-cost and scalable	Poor controllability and stability	[22]
Porous AMs	Yes	NA	Fast ions transport, high active surface area, supporting high power density	Sacrificing energy density, increasing manufacturing cost and mechanical instability	[33–35]
Pore additives	Yes	NA	Fast ions transport in thick electrodes, scalable, supporting high energy and power densities	More manufacturing steps and increased cost	[58–61]
Additive manufacturing	Yes	NA	Programmable control of electrode configuration	Low manufacturing efficiency, limited application	[62–65]
Core–shell AMs	NA	Yes	Stable and uniform, supporting high energy and power densities	Poor scalability and high materials cost	[93–95,122]
Conductive wrapping	NA	Yes	Deformation-tolerant, supporting high power density	Poor scalability and high cost	[161–165]
Conductive binders	NA	Yes	Stable and uniform, supporting high energy density	Poor scalability and high materials cost	[181,182]
Structural binders	NA	Yes	Stable and uniform ETN, good mechanical flexibility	Nonactive, sacrificing energy density	[192–194]
Electrode templates	Yes	Yes	Precise control of ITN and ETN, supporting high power density	Poor scalability, limitation in AMs, and high cost	[216–223]
Electrode scaffolds	Yes	Yes	Mechanical flexibility and strength, robust ITN and ETN, supporting high power density, long cycle stability	Low energy density, high cost, limitation in AMs	[228,261,262]
Electrode matrix	Yes	Yes	Mechanical flexibility, uniform and stable ITN and ETN	Limitation in energy and power densities	[289]

Note: NA—not applicable.

strategies is the modification of AMs, including core–shell design of AMs, flexible wrapping of AMs by conductive agents, and conductive binder coating. The most significant advantage of these strategies is that they can reinforce, uniformize, and stabilize the connection between AMs and ETN with a very small amount of conductive agent. This is critical for maintaining a high energy density. The main disadvantages are probably the high cost in manufacturing, type limitation of AMs, etc. The second group of strategies for ETN control is the binder engineering to reinforce the interfaces among AMs, conductive fillers and current collectors, in order to achieve good structural and conductive stability for the ETN. As introduced in the section of structural binders, strong adhesion and mechanical properties of binders play a key role in determining the structural uniformity, stability and flexibility of the whole composite electrode and so the ETN/ITN structures. The third group of strategies is the structural conductive materials which have been employed as electrode scaffolds or template, such as porous carbon frame and metal foams. One big advantage is that these structural conductive materials can provide not only a mechanically strong and/or flexible ETN, but also orientated and/or large ions-transport channels for fast ion-transport. However, the disadvantages are also obvious, for example, the notable loss of energy density, poor scalability, and high cost, etc. For future studies on ITN control, the key is to achieve stable and uniform ETN/AM contact, good mechanical properties and even multifunction for the binder/conductive agent composite, with nonactive materials as less as possible.

5.2. Challenges and Perspectives

With the development of ESDs, there are increasing demands on high energy and power densities, long-term cycle stability,

good safety and even mechanical flexibility, with all at a low cost. Clearly, a robust charge transport system is one of the primary keys for achieving these performances. Therefore, a comprehensive understanding of the challenges for the charge transport system (particularly the physical transport networks as summarized in this review) and their relationships with the desired device performances is critical for the success of next generation ESDs. As illustrated in **Figure 19**, the relationships among charge transport system, AMs and device performance, and the possible challenges for building robust charge transport system in composite electrodes, are summarized in one picture. The ETN, the ITN, and the AMs provide the basic support for the “wish-list bridge” of device performances. It should be noted that there is almost no ideal ESD that can satisfy all the requirements as shown in **Figure 19**. Therefore, the challenges for ETN/ITN control depend on the specific application.

Challenges on Component Level: On material component level, the main challenge is to simultaneously realize desired material functions (such as conduction, lithium ion storage), appropriate mechanical and interfacial properties, and rational morphology with good uniformity. These structures and properties are the key factors shaping the charge transport networks in composite electrodes. This challenge applies to all the primary components in ESDs, including electrolytes, active materials, conductive agent, binders, etc. For example, for liquid electrolytes, although mechanical properties are seldom discussed, the trade-off between ion-conductivity and viscosity is also well known.^[296–298] It is easy to understand that good mechanical properties of an electrolyte will help to stabilize the structures of composite electrodes, and so the charge transport networks. Therefore, solid polymer electrolytes,^[299–303] and ceramic solid electrolytes,^[304–308] are

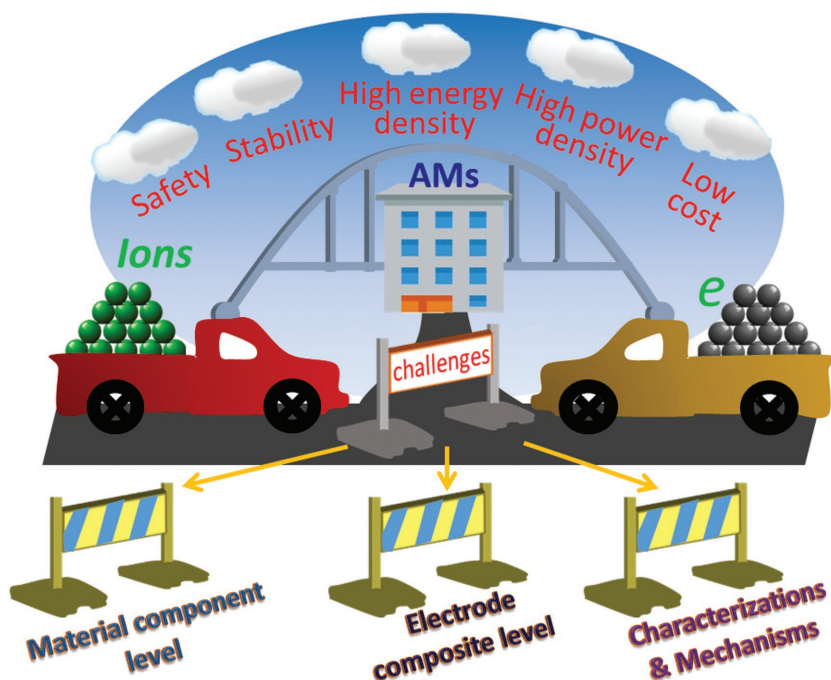


Figure 19. A big picture showing the challenges for building a robust charge transport system for advanced energy storage devices. The two physical networks (ITN and ETN) and AMs are the most fundamental support for the “wish bridge.” The main challenges come from the limitation and competition from space and weight, limited functions/properties of individual component, the coupling effect between electrochemistry and mechanics, a poor understanding of the structures-properties-performance relationships on both materials and cell levels, etc. For details, please see the text.

promising solutions to build mechanically strong ITN inside the electrodes. For ETN, similar challenge exists for both binder and conductive agent. For example, binders are usually nonconductive and conductive agents are weak in interface interactions. As a result, the ETN built by the two usually suffers from either insufficient electronic conductivity or weak mechanical properties. To address this challenge, structural AMs, adhesive and conductive binders, surface treatment of components to achieve better adhesion are possible solutions. It is noted that the solvent in the electrode slurry also plays a critical role in controlling the interactions among polymer binders, conductive fillers and AMs particles as revealed recently by Zhong and co-workers.^[309]

Challenges on Composite Electrode Level: The challenges on composite electrode level depend on the specific requirements on device performance and properties. For example, if high energy density, high power density, and/or long cycle stability are required, the biggest challenge comes from the space and weight competition between the charge transport system (i.e., the ITN and ETN) and AMs. This challenge is fundamentally due to the fact that high energy density requires a high volume or weight percentage of AMs, similarly, a high power density needs a high volume percentage of charge transport system in the composite electrodes. They cannot be satisfied simultaneously in a fixed volume. It seems that there is no fundamental solution to this issue. However, a rational design of the structures of electrode

composite with high-capacity AMs can be the most promising solution for this issue. This is because higher capacity AMs can improve the energy density with even lower loading as compared with traditional low-capacity AMs, which can make more space for the charge transport system. However, the success depends on whether one can solve the instability issues of charge transport networks with the big-volume-change or dissolution of AMs as introduced previously.

Challenges in Characterizations, Understanding, and Simulation: As introduced previously, the 3D structures of ETN and ITN are complicated, but they play a pivotal role in controlling the overall performance of ESDs. Therefore, characterizations of the structures and properties of the charge transport networks and tracking their evolution during practice is very critical for understanding the performance and its decay behavior. As far as we know, there is lack of experimental method for direct study on the ionic conductivity of wet composite electrodes. The conventional way for this is the Electrochemical Impedance Spectroscopy (EIS) analysis or C-rate performance testing of the assembled battery cell. Generally, the ionic conductivity of electrode is determined by two critical factors: the structures of ITN and the ion-conductivity of electrolyte. For electrical

conductivity, conventional methods, such as resistivity testing by four-probe method,^[310] have been widely used for both dry and wet electrodes. It is important to separately characterize the ionic and electronic conductivities, which is critical for a better understanding of the property-performance relationship for composite electrodes. In this case, models on how the porous structures (ITN structure) determine the ion transport inside composite electrodes are very helpful. For example, Terao et al. proposed a numerical calculation equation as shown below to describe the mass transport properties of porous electrode^[311]

$$D^R = \frac{D^{\text{eff}}}{D^{\text{bulk}}} = \frac{\varepsilon}{\tau} = 1 / (1 + D^{\text{bulk}} / D^k) \quad (1)$$

$$D^k = \frac{2}{3} (8RT / \pi M)^{1/2} r \quad (2)$$

where, D^R is the relative diffusion coefficient, ε is porosity, τ is tortuosity, and r is pore radius. These parameters were obtained from the reconstructed structure of the porous electrode. D^k is the Knudsen diffusion coefficient. It is noted that these values are very helpful to describe the average properties of electrodes, but not the uniformity of electrode properties. Therefore, there is a big challenge of evaluating the uniformity of charge transport properties inside the porous electrode, which plays a critical role in controlling

the uniformity of local current, the cycle stability and safety of the device.

However, we believe that, with the development of simulation technology and characterization techniques, it is absolutely possible to realize theoretical prediction on the electrochemical performance of composite electrodes. Although the progress in this field is sluggish, there are significant studies worthy of discussion. For example, recently, Wood and co-workers developed a model to describe how materials factors, SEI, and adhesion among components impact the detachment of AMs from conductive networks and the capacity fade, which is instructive for design of better conductive networks for high-capacity AMs.^[312] There are also earlier pioneering efforts. For instance, Park and co-workers developed a model to include multiscale and multiphysics phenomena in composite electrode.^[313] The developed model has revealed complicated dynamic electrochemical behaviors related to the variation of particle shape, tortuosity, material composition, etc. For thick composite electrodes, the theoretical studies become even more challenging but critical for the optimization and practical application. A very significant effort on this point was reported by Inoue and Kawase.^[314] In this study, they developed a correlation equation between a porous structure and the effective conductivity. They found that the binder distribution and the particle morphology are the most dominant factors that degrade ion transportation in thick electrodes. Another significant effort on the theoretical studies of thick electrode was reported by Danner and co-workers,^[315] which describes a detailed 3D microstructure resolved model to investigate limiting factors for battery performance. In short, more theoretical studies are in critical need, and the characterizations and understanding of multiscale, multiphysical, electro-chemo-mechanical problems are the main challenges for simulation studies.^[316–318]

In conclusion, building advanced “traffic system” for charge transport has been a critical and primary task for the R&D of next-generation ESDs with especially high-capacity AMs. The construction of robust “traffic system” highly depends on a good team work among active materials, electrolytes, conductive agents, polymer binders, manufacturing, and cell assembly. At the same time, characterizations of the ETN/ITN structures/properties and a better understanding their roles at electrode and cell levels are in critical and urgent need by advanced ESDs.

Acknowledgements

This work was supported by the National Science Foundation under award number NSF-1463616, and by the WA JCATI project titled “A Gummy Electrolyte with Damage-tolerance and Thermal-protection Capabilities for Safer Li-ion Batteries.”

Conflict of Interest

The authors declare no conflict of interest.

Keywords

electrical vehicles, high-capacity electrodes, lithium–sulfur batteries, microstructure control, silicon

Received: July 2, 2018

Revised: August 24, 2018

Published online: December 17, 2018

- [1] B. Dunn, H. Kamath, J. M. Tarascon, *Science* **2011**, 334, 928.
- [2] Y. Jin, B. Zhu, Z. D. Lu, N. Liu, J. Zhu, *Adv. Energy Mater.* **2017**, 7, 1700715.
- [3] S. T. Taleghani, B. Marcos, K. Zaghbi, G. Lantagne, *J. Electrochem. Soc.* **2017**, 164, E3179.
- [4] S. Cho, C. F. Chen, P. P. Mukherjee, *J. Electrochem. Soc.* **2015**, 162, A1202.
- [5] Z. Y. Jiang, Z. G. Qu, L. Zhou, W. Q. Tao, *Appl. Energy* **2017**, 194, 530.
- [6] D. R. Neversa, S. W. Peterson, L. Robertson, C. Chubbuck, J. Flygare, K. Cole, D. R. Wheeler, *J. Electrochem. Soc.* **2014**, 161, A1691.
- [7] M. A. Sadeghi, M. Aghighi, J. Barralet, J. T. Gostick, *Chem. Eng. J.* **2017**, 330, 1002.
- [8] M. A. Munoz-Marquez, D. Saurel, J. L. Gomez-Camer, M. Casas-Cabanias, E. Castillo-Martinez, T. Rojo, *Adv. Energy Mater.* **2017**, 7, 1700463.
- [9] P. Verma, P. Maire, P. Novak, *Electrochim. Acta* **2010**, 55, 6332.
- [10] P. Schwager, H. Bulter, I. Plettenberg, G. Wittstock, *Energy Technology* **2016**, 4, 1472.
- [11] Y. Oh, S. Nam, S. Wi, S. Hong, B. Park, *Electron. Mater. Lett.* **2012**, 8, 91.
- [12] C. P. Yang, Y. G. Yao, S. M. He, H. Xie, E. Hitz, L. B. Hu, *Adv. Mater.* **2017**, 29, 1702714.
- [13] N. Weber, P. Beckstein, W. Herremann, G. M. Horstmann, C. Nore, F. Stefani, T. Weier, *Phys. Fluids* **2017**, 29, 054101.
- [14] L. H. Ye, W. Q. Lv, J. Y. Cui, Y. C. Liang, P. Wu, X. N. Wang, H. He, S. J. Lin, W. Wang, J. H. Dickerson, W. D. He, *ChemElectroChem* **2015**, 2, 312.
- [15] C. H. Huang, S. X. Zhuang, F. Y. Tu, *J. Electrochem. Soc.* **2013**, 160, A376.
- [16] Y. F. Yuan, K. Amine, J. Lu, R. Shahbazian-Yassar, *Nat. Commun.* **2017**, 8, 15806.
- [17] X. P. Li, C. L. Yan, J. N. Wang, A. Graff, S. L. Schweizer, A. Sprafke, O. G. Schmidt, R. B. Wehrspohn, *Adv. Energy Mater.* **2015**, 5, 1401556.
- [18] X. F. Tang, G. W. Wen, Y. Song, *Appl. Surf. Sci.* **2018**, 436, 398.
- [19] J. Q. Zhou, T. Qian, M. F. Wang, N. Xu, Q. Zhang, Q. Li, C. L. Yan, *ACS Appl. Mater. Interfaces* **2016**, 8, 5358.
- [20] G. Liu, H. Zheng, X. Song, V. S. Battaglia, *J. Electrochem. Soc.* **2012**, 159, A214.
- [21] M. M. Forouzan, M. Wray, L. Robertson, D. R. Wheeler, *J. Electrochem. Soc.* **2017**, 164, A3117.
- [22] A. Kraysberg, Y. Ein-Eli, *Adv. Energy Mater.* **2016**, 6, 1600655.
- [23] G. F. Yang, S. K. Joo, *Electrochim. Acta* **2015**, 170, 263.
- [24] H. H. Zheng, L. Tan, G. Liu, X. Y. Song, V. S. Battaglia, *J. Power Sources* **2012**, 208, 52.
- [25] H. X. Kang, C. Lim, T. Y. Li, Y. Z. Fu, B. Yan, N. Houston, V. De Andrade, F. De Carlo, L. K. Zhu, *Electrochim. Acta* **2017**, 232, 431.
- [26] C. Lim, B. Yan, H. X. Kang, Z. B. Song, W. C. Lee, V. De Andrade, F. De Carlo, L. L. Yin, Y. Kim, L. K. Zhu, *J. Power Sources* **2016**, 328, 46.
- [27] B. Delattre, R. Amin, J. Sander, J. De Coninck, A. P. Tomsia, Y. M. Chiang, *J. Electrochem. Soc.* **2018**, 165, A388.
- [28] J. Illig, M. Ender, T. Chrobak, J. P. Schmidt, D. Klotz, E. Ivers-Tiffée, *J. Electrochem. Soc.* **2012**, 159, A952.

- [29] A. van Bommel, R. Divigalpitaya, *J. Electrochem. Soc.* **2012**, *159*, A1791.
- [30] D. P. Lv, J. M. Zheng, Q. Y. Li, X. Xie, S. Ferrara, Z. M. Nie, L. B. Mehdi, N. D. Browning, J. G. Zhang, G. L. Graff, J. Liu, J. Xiao, *Adv. Energy Mater.* **2015**, *5*, 1402290.
- [31] S. Rehman, K. Khan, Y. F. Zhao, Y. L. Hou, *J. Mater. Chem. A* **2017**, *5*, 3014.
- [32] Y. X. Yin, H. R. Yao, Y. G. Guo, *Chin. Phys. B* **2016**, *25*, 018801.
- [33] Y. Cai, H. E. Wang, X. Zhao, F. Huang, C. Wang, Z. Deng, Y. Li, G. Z. Cao, B. L. Su, *ACS Appl. Mater. Interfaces* **2017**, *9*, 10652.
- [34] M. H. Park, K. Kim, J. Kim, J. Cho, *Adv. Mater.* **2010**, *22*, 415.
- [35] H. Yoo, M. Jo, B. S. Jin, H. S. Kim, J. Cho, *Adv. Energy Mater.* **2011**, *1*, 347.
- [36] J. Lee, Y. M. Chen, Y. Zhu, B. D. Vogt, *ACS Appl. Mater. Interfaces* **2014**, *6*, 21011.
- [37] B. M. Bang, J. I. Lee, H. Kim, J. Cho, S. Park, *Adv. Energy Mater.* **2012**, *2*, 878.
- [38] V. Etacheri, G. A. Seisenbaeva, J. Caruthers, G. Daniel, J. M. Nedelec, V. G. Kessler, V. G. Pol, *Adv. Energy Mater.* **2015**, *5*, 1401289.
- [39] G. Y. Xu, B. Ding, P. Nie, L. F. Shen, J. Wang, X. G. Zhang, *Chem. – Eur. J.* **2013**, *19*, 12306.
- [40] Q. F. Xiao, M. Gu, H. Yang, B. Li, C. M. Zhang, Y. Liu, F. Liu, F. Dai, L. Yang, Z. Y. Liu, X. C. Xiao, G. Liu, P. Zhao, S. L. Zhang, C. M. Wang, Y. F. Lu, M. Cai, *Nat. Commun.* **2015**, *6*, 8844.
- [41] A. Magasinski, P. Dixon, B. Hertzberg, A. Kvit, J. Ayala, G. Yushin, *Nat. Mater.* **2010**, *9*, 353.
- [42] N. Liu, Z. D. Lu, J. Zhao, M. T. McDowell, H. W. Lee, W. T. Zhao, Y. Cui, *Nat. Nanotechnol.* **2014**, *9*, 187.
- [43] H. B. Geng, S. S. Li, Y. Pan, Y. G. Yang, J. W. Zheng, H. W. Gu, *RSC Adv.* **2015**, *5*, 52993.
- [44] C. M. Doherty, R. A. Caruso, B. M. Smarsly, P. Adelhelm, C. J. Drummond, *Chem. Mater.* **2009**, *21*, 5300.
- [45] C. M. Doherty, R. A. Caruso, B. M. Smarsly, C. J. Drummond, *Chem. Mater.* **2009**, *21*, 2895.
- [46] Q. Fan, L. X. Lei, Y. M. Sun, *Nanoscale* **2014**, *6*, 7188.
- [47] P. C. Lian, J. Y. Wang, D. D. Cai, G. X. Liu, Y. Y. Wang, H. H. Wang, *J. Alloys Compd.* **2014**, *604*, 188.
- [48] A. K. Mondal, K. Kretschmer, Y. F. Zhao, H. Liu, C. Y. Wang, B. Sun, G. X. Wang, *Chem. – Eur. J.* **2017**, *23*, 3683.
- [49] A. Vu, Y. Q. Qian, A. Stein, *Adv. Energy Mater.* **2012**, *2*, 1056.
- [50] J. Q. Wang, G. D. Du, R. Zeng, B. Niu, Z. X. Chen, Z. P. Guo, S. X. Dou, *Electrochim. Acta* **2010**, *55*, 4805.
- [51] M. J. Choi, Y. Xiao, J. Y. Hwang, I. Belharouak, Y. K. Sun, *J. Power Sources* **2017**, *348*, 302.
- [52] H. I. Park, M. Sohn, D. S. Kim, C. Park, J. H. Choi, H. Kim, *ChemSusChem* **2016**, *9*, 834.
- [53] B. Z. Yu, X. L. Liu, H. G. Zhang, G. Y. Jing, P. Ma, Y. N. Luo, W. M. Xue, Z. Y. Ren, H. M. Fan, *J. Mater. Chem. A* **2015**, *3*, 16544.
- [54] C. C. Lin, Y. C. Yen, H. C. Wu, N. L. Wu, *J. Chin. Chem. Soc.* **2012**, *59*, 1226.
- [55] S. W. Oh, S. T. Myung, S. M. Oh, K. H. Oh, K. Amine, B. Scrosati, Y. K. Sun, *Adv. Mater.* **2010**, *22*, 4842.
- [56] J. L. Cheng, G. F. Gu, Q. Guan, J. M. Razal, Z. Y. Wang, X. L. Li, B. Wang, *J. Mater. Chem. A* **2016**, *4*, 2729.
- [57] H. Uchlyama, E. Hosono, I. Honma, H. Zhou, H. Imai, *Electrochem. Commun.* **2008**, *10*, 52.
- [58] J. S. Sander, R. M. Erb, L. Li, A. Gurijala, Y. M. Chiang, *Nat. Energy* **2016**, *1*, 16099.
- [59] R. Elango, A. Demortière, V. D. Andrade, M. Morcrette, V. Seznec, *Adv. Energy Mater.* **2018**, 1703031.
- [60] G. Ai, Y. L. Dai, W. F. Mao, H. Zhao, Y. B. Fu, X. Y. Song, Y. F. En, V. S. Battaglia, V. Srinivasan, G. Liu, *Nano Lett.* **2016**, *16*, 5365.
- [61] H. Zhao, Q. Yang, N. Yuca, M. Ling, K. Higa, V. S. Battaglia, D. Y. Parkinson, V. Srinivasan, G. Liu, *Nano Lett.* **2016**, *16*, 4686.
- [62] K. Shen, H. L. Mei, B. Li, J. W. Ding, S. B. Yang, *Adv. Energy Mater.* **2018**, *8*, 1701527.
- [63] J. T. Hu, Y. Jiang, S. H. Cui, Y. D. Duan, T. C. Liu, H. Guo, L. P. Lin, Y. Lin, J. X. Zheng, K. Amine, F. Pan, *Adv. Energy Mater.* **2016**, *6*, 1600856.
- [64] D. Bradley, *Mater. Today* **2013**, *16*, 256.
- [65] K. Fu, Y. B. Wang, C. Y. Yan, Y. G. Yao, Y. A. Chen, J. Q. Dai, S. Lacey, Y. B. Wang, J. Y. Wan, T. Li, Z. Y. Wang, Y. Xu, L. B. Hu, *Adv. Mater.* **2016**, *28*, 2587.
- [66] J. Li, M. C. Leu, R. Panat, J. Park, *Mater. Des.* **2017**, *119*, 417.
- [67] Y. B. Wang, C. J. Chen, H. Xie, T. T. Gao, Y. G. Yao, G. Pastel, X. G. Han, Y. J. Li, J. P. Zhao, K. Fu, L. B. Hu, *Adv. Funct. Mater.* **2017**, *27*, 1703140.
- [68] C. W. Foster, M. P. Down, Y. Zhang, X. B. Ji, S. J. Rowley-Neale, G. C. Smith, P. J. Kelly, C. E. Banks, *Sci. Rep.* **2017**, *7*, 42233.
- [69] K. Sun, T. S. Wei, B. Y. Ahn, J. Y. Seo, S. J. Dillon, J. A. Lewis, *Adv. Mater.* **2013**, *25*, 4539.
- [70] X. C. Tian, J. Jin, S. Q. Yuan, C. K. Chua, S. B. Tor, K. Zhou, *Adv. Energy Mater.* **2017**, *7*, 1700127.
- [71] L. F. Arenas, F. C. Walsh, C. P. de Leon, *ECS J. Solid State Sci. Technol.* **2015**, *4*, P3080.
- [72] J. Marschewski, L. Brenner, N. Ebejer, P. Ruch, B. Michel, D. Poulidakos, *Energy Environ. Sci.* **2017**, *10*, 780.
- [73] K. Percin, A. Rommerskirchen, R. Sengpiel, Y. Gendel, M. Wessling, *J. Power Sources* **2018**, *379*, 228.
- [74] F. Zhang, M. Wei, V. V. Viswanathan, B. Swart, Y. Y. Shao, G. Wu, C. Zhou, *Nano Energy* **2017**, *40*, 418.
- [75] C. Zhu, T. Y. Liu, F. Qian, W. Chen, S. Chandrasekaran, B. Yao, Y. Song, E. B. Duoss, J. D. Kuntz, C. M. Spadaccini, M. A. Worsley, Y. Li, *Nano Today* **2017**, *15*, 107.
- [76] K. Fu, Y. G. Yao, J. Q. Dai, L. B. Hu, *Adv. Mater.* **2017**, *29*, 1603486.
- [77] F. Sauvage, J. M. Tarascon, E. Baudrin, *J. Phys. Chem. C* **2007**, *111*, 9624.
- [78] J. B. Bates, N. J. Dudney, B. J. Neudecker, F. X. Hart, H. P. Jun, S. A. Hackney, *J. Electrochem. Soc.* **2000**, *147*, 59.
- [79] H. G. Zhang, H. Ning, J. Busbee, Z. H. Shen, C. Kiggins, Y. Hua, J. Eaves, J. Davis, T. Shi, Y. T. Shao, J. M. Zuo, X. H. Hong, Y. Chan, S. B. Wang, P. Wang, P. C. Sun, S. Xu, J. Liu, P. V. Braun, *Sci. Adv.* **2017**, *3*, e1602427.
- [80] N. Delpuech, N. Dupre, P. Moreau, J. S. Bridel, J. Gaubicher, B. Lestriez, D. Guyomard, *ChemSusChem* **2016**, *9*, 841.
- [81] T. Waldmann, S. Gorse, T. Samtleben, G. Schneider, V. Knoblauch, M. Wohlfahrt-Mehrens, *J. Electrochem. Soc.* **2014**, *161*, A1742.
- [82] J. Vetter, P. Novak, M. R. Wagner, C. Veit, K. C. Moller, J. O. Besenhard, M. Winter, M. Wohlfahrt-Mehrens, C. Vogler, A. Hammouche, *J. Power Sources* **2005**, *147*, 269.
- [83] M. Ko, S. Chae, J. Cho, *ChemElectroChem* **2015**, *2*, 1645.
- [84] D. L. Ma, Z. Y. Cao, A. M. Hu, *Nano-Micro Lett.* **2014**, *6*, 347.
- [85] W. Y. Li, Q. F. Zhang, G. Y. Zheng, Z. W. Seh, H. B. Yao, Y. Cui, *Nano Lett.* **2013**, *13*, 5534.
- [86] W. D. Zhou, X. C. Xiao, M. Cai, L. Yang, *Nano Lett.* **2014**, *14*, 5250.
- [87] C. Wang, F. Luo, H. Lu, X. H. Rong, B. N. Liu, G. Chu, Y. Sun, B. G. Quan, J. Y. Zheng, J. J. Li, C. Z. Gu, X. P. Qiu, H. Li, L. Q. Chen, *ACS Appl. Mater. Interfaces* **2017**, *9*, 2806.
- [88] H. S. Choi, S. J. Kim, H. W. Choi, C. E. Park, Y. J. Gao, Y. Hang, S. Y. Jeong, J. P. Kim, J. S. Bae, C. R. Cho, *Curr. Appl. Phys.* **2017**, *17*, 1087.
- [89] S. Q. Chen, L. F. Shen, P. A. van Aken, J. Maier, Y. Yu, *Adv. Mater.* **2017**, *29*, 1605650.
- [90] M. G. Jeong, M. Islam, H. L. Du, Y. S. Lee, H. H. Sun, W. Choi, J. K. Lee, K. Y. Chung, H. G. Jung, *Electrochim. Acta* **2016**, *209*, 299.
- [91] L. Y. Yang, H. Z. Li, J. Liu, Z. Q. Sun, S. S. Tang, M. Lei, *Sci. Rep.* **2015**, *5*, 10908.
- [92] J. S. Kim, M. Halim, D. Byun, J. K. Lee, *Solid State Ionics* **2014**, *260*, 36.

- [93] L. Cheng, J. Yan, G. N. Zhu, J. Y. Luo, C. X. Wang, Y. Y. Xia, *J. Mater. Chem.* **2010**, *20*, 595.
- [94] C. B. Zhu, Y. Yu, L. Gu, K. Weichert, J. Maier, *Angew. Chem., Int. Ed.* **2011**, *50*, 6278.
- [95] T. Okubo, T. Yamada, M. Saito, C. Yodoya, A. Kamei, M. Hirota, T. Takenaka, A. Tasaka, M. Inaba, *Electrochemistry* **2012**, *80*, 720.
- [96] M. N. He, Q. Sa, G. Liu, Y. Wang, *ACS Appl. Mater. Interfaces* **2013**, *5*, 11152.
- [97] Z. D. Lu, N. Liu, H. W. Lee, J. Zhao, W. Y. Li, Y. Z. Li, Y. Cui, *ACS Nano* **2015**, *9*, 2540.
- [98] Y. Jiang, Z. Z. Yang, W. H. Li, L. C. Zeng, F. S. Pan, M. Wang, X. Wei, G. T. Hu, L. Gu, Y. Yu, *Adv. Energy Mater.* **2015**, *5*, 1402104.
- [99] E. Kang, Y. S. Jung, G. H. Kim, J. Chun, U. Wiesner, A. C. Dillon, J. K. Kim, J. Lee, *Adv. Funct. Mater.* **2011**, *21*, 4349.
- [100] Y. W. Cheng, C. K. Lin, Y. C. Chu, A. Abouimrane, Z. H. Chen, Y. Ren, C. P. Liu, Y. H. Tzeng, O. Auciello, *Adv. Mater.* **2014**, *26*, 3724.
- [101] S. Lee, Y. Cho, H. K. Song, K. T. Lee, J. Cho, *Angew. Chem., Int. Ed.* **2012**, *51*, 8748.
- [102] H. Kim, H. Kim, S. W. Kim, K. Y. Park, J. Kim, S. Jeon, K. Kang, *Carbon* **2012**, *50*, 1966.
- [103] J. J. Wang, X. L. Sun, *Energy Environ. Sci.* **2012**, *5*, 5163.
- [104] S. A. Klankowski, R. A. Rojeski, B. A. Cruden, J. W. Liu, J. Wu, J. Li, *J. Mater. Chem. A* **2013**, *1*, 1055.
- [105] Z. L. Xu, Y. Gang, M. A. Garakani, S. Abouali, J. Q. Huang, J. K. Kim, *J. Mater. Chem. A* **2016**, *4*, 6098.
- [106] B. A. Zhang, Z. D. Huang, S. W. Oh, J. K. Kim, *J. Power Sources* **2011**, *196*, 10692.
- [107] R. G. Ford, *MRS Bull.* **2007**, *32*, 755.
- [108] I. D. Scott, Y. S. Jung, A. S. Cavanagh, Y. F. An, A. C. Dillon, S. M. George, S. H. Lee, *Nano Lett.* **2011**, *11*, 414.
- [109] W. H. Li, M. S. Li, Z. Z. Yang, J. Xu, X. W. Zhong, J. Q. Wang, L. C. Zeng, X. W. Liu, Y. Jiang, X. Wei, L. Gu, Y. Yu, *Small* **2015**, *11*, 2762.
- [110] X. Han, H. X. Chen, J. J. Liu, H. H. Liu, P. Wang, K. Huang, C. Li, S. Y. Chen, Y. Yang, *Electrochim. Acta* **2015**, *156*, 11.
- [111] Q. Sun, B. He, X. Q. Zhang, A. H. Lu, *ACS Nano* **2015**, *9*, 8504.
- [112] J. Moskon, R. Dominko, R. Cerc-Korosec, M. Gaberscek, J. Jamnik, *J. Power Sources* **2007**, *174*, 683.
- [113] L. F. Shen, H. S. Li, E. Uchaker, X. G. Zhang, G. Z. Cao, *Nano Lett.* **2012**, *12*, 5673.
- [114] Z. Favors, H. H. Bay, Z. Mutlu, K. Ahmed, R. Ionescu, R. Ye, M. Ozkan, C. S. Ozkan, *Sci. Rep.* **2015**, *5*, 8246.
- [115] D. Gueon, J. Lee, J. K. Lee, J. H. Moon, *RSC Adv.* **2016**, *6*, 38012.
- [116] H. F. Ni, J. K. Liu, L. Z. Fan, *Nanoscale* **2013**, *5*, 2164.
- [117] Y. G. Wang, Y. R. Wang, E. J. Hosono, K. X. Wang, H. S. Zhou, *Angew. Chem., Int. Ed.* **2008**, *47*, 7461.
- [118] N. Li, G. M. Zhou, F. Li, L. Wen, H. M. Cheng, *Adv. Funct. Mater.* **2013**, *23*, 5429.
- [119] Y. B. He, F. Ning, B. H. Li, Q. S. Song, W. Lv, H. D. Du, D. Y. Zhai, F. Y. Su, Q. H. Yang, F. Y. Kang, *J. Power Sources* **2012**, *202*, 253.
- [120] X. Li, J. Xu, P. X. Huang, W. Yang, Z. Q. Wang, M. S. Wang, Y. Huang, Y. Zhou, M. Z. Qu, Z. L. Yu, Y. H. Lin, *Electrochim. Acta* **2016**, *190*, 69.
- [121] H. Choi, C. C. Nguyen, S. W. Song, *Bull. Korean Chem. Soc.* **2010**, *31*, 2519.
- [122] T. M. Higgins, S. H. Park, P. J. King, C. Zhang, N. MoEvoy, N. C. Berner, D. Daly, A. Shmeliov, U. Khan, G. Duesberg, V. Nicolosi, J. N. Coleman, *ACS Nano* **2016**, *10*, 3702.
- [123] X. Sun, Q. Li, Y. B. Mao, *Electrochim. Acta* **2015**, *174*, 563.
- [124] Y. R. Li, L. X. Yuan, Z. Li, Y. Z. Qi, C. Wu, J. Liu, Y. H. Huang, *RSC Adv.* **2015**, *5*, 44160.
- [125] Y. Yao, N. Liu, M. T. McDowell, M. Pasta, Y. Cui, *Energy Environ. Sci.* **2012**, *5*, 7927.
- [126] Y. L. Zhou, Y. L. Li, J. Yang, J. Tian, H. Y. Xu, J. Yang, W. L. Fan, *ACS Appl. Mater. Interfaces* **2016**, *8*, 18797.
- [127] Y. Z. Fu, A. Manthiram, *RSC Adv.* **2012**, *2*, 5927.
- [128] Y. H. Huang, J. B. Goodenough, *Chem. Mater.* **2008**, *20*, 7237.
- [129] J. Z. Wang, L. Lu, D. Q. Shi, R. Tandiono, Z. X. Wang, K. Konstantinov, H. K. Liu, *ChemPlusChem* **2013**, *78*, 318.
- [130] T. Wang, W. Wang, D. Zhu, L. W. Huang, Y. G. Chen, *Mater. Res. Bull.* **2015**, *71*, 91.
- [131] G. W. Yoo, B. C. Jang, S. G. Min, J. T. Son, *J. Nanosci. Nanotechnol.* **2016**, *16*, 2637.
- [132] G. H. Yuan, H. D. Wang, *J. Energy Chem.* **2014**, *23*, 657.
- [133] L. Zhan, H. B. Chen, J. Q. Fang, S. Q. Wang, L. X. Ding, Z. Li, P. J. Ashman, H. H. Wang, *Electrochim. Acta* **2016**, *209*, 192.
- [134] X. W. Gao, J. Z. Wang, S. L. Chou, H. K. Liu, *J. Power Sources* **2012**, *220*, 47.
- [135] H. Y. Lin, C. H. Li, D. Y. Wang, C. C. Chen, *Nanoscale* **2016**, *8*, 1280.
- [136] S. Moon, Y. H. Jung, D. K. Kim, *J. Power Sources* **2015**, *294*, 386.
- [137] H. Y. Yan, W. X. Chen, X. M. Wu, Y. F. Li, *Electrochim. Acta* **2014**, *146*, 295.
- [138] Y. Yang, G. H. Yu, J. J. Cha, H. Wu, M. Vosgueritchian, Y. Yao, Zn Bao, Y. Cui, *ACS Nano* **2011**, *5*, 9187.
- [139] X. Y. Zhou, F. Chen, J. Yang, *J. Energy Chem.* **2015**, *24*, 448.
- [140] Y. H. Cao, D. Fang, X. Q. Liu, Z. P. Luo, G. Z. Li, W. L. Xu, M. Jiang, C. X. Xiong, *Compos. Sci. Technol.* **2016**, *137*, 130.
- [141] R. Q. Liu, D. Y. Li, C. Wang, N. Li, Q. Li, X. J. Lu, J. S. Spendelov, G. Wu, *Nano Energy* **2014**, *6*, 73.
- [142] J. H. Kong, W. A. Yee, Y. F. Wei, L. P. Yang, J. M. Ang, S. L. Phua, S. Y. Wong, R. Zhou, Y. L. Dong, X. Li, X. H. Lu, *Nanoscale* **2013**, *5*, 2967.
- [143] N. Li, S. X. Jin, Q. Y. Liao, H. Cu, C. X. Wang, *Nano Energy* **2014**, *5*, 105.
- [144] D. Nan, Z. H. Huang, R. T. Lv, Y. X. Lin, L. Yang, X. L. Yu, L. Ye, W. C. Shen, H. Y. Sun, F. Y. Kang, *J. Nanomater.* **2014**, *2014*, 1.
- [145] M. Sangare, G. J. Fodjouong, X. T. Huang, *Mendeleev Commun.* **2013**, *23*, 284.
- [146] H. C. Tao, X. L. Yang, L. L. Zhang, S. B. Ni, *J. Solid State Electrochem.* **2014**, *18*, 1989.
- [147] H. W. Yue, S. Y. Wang, Z. B. Yang, Q. Li, S. M. Lin, D. Y. He, *Electrochim. Acta* **2015**, *174*, 688.
- [148] S. Q. Chen, X. D. Huang, B. Sun, J. Q. Zhang, H. Liu, G. X. Wang, *J. Mater. Chem. A* **2014**, *2*, 16199.
- [149] Y. M. Chen, X. Y. Li, K. S. Park, J. H. Hong, J. Song, L. M. Zhou, Y. W. Mai, H. T. Huang, J. B. Goodenough, *J. Mater. Chem. A* **2014**, *2*, 10126.
- [150] N. Jayaprakash, J. Shen, S. S. Moganty, A. Corona, L. A. Archer, *Angew. Chem., Int. Ed.* **2011**, *50*, 5904.
- [151] W. Y. Li, G. Y. Zheng, Y. Yang, Z. W. Seh, N. Liu, Y. Cui, *Proc. Natl. Acad. Sci. USA* **2013**, *110*, 7148.
- [152] C. F. Zhang, H. B. Wu, C. Z. Yuan, Z. P. Guo, X. W. Lou, *Angew. Chem., Int. Ed.* **2012**, *51*, 9592.
- [153] Y. Zhao, W. L. Wu, J. X. Li, Z. C. Xu, L. H. Guan, *Adv. Mater.* **2014**, *26*, 5113.
- [154] G. Y. Zheng, Y. Yang, J. J. Cha, S. S. Hong, Y. Cui, *Nano Lett.* **2011**, *11*, 4462.
- [155] G. Y. Zheng, Q. F. Zhang, J. J. Cha, Y. Yang, W. Y. Li, Z. W. Seh, Y. Cui, *Nano Lett.* **2013**, *13*, 1265.
- [156] S. Li, J. J. Niu, Y. C. Zhao, K. P. So, C. Wang, C. A. Wang, J. Li, *Nat. Commun.* **2015**, *6*, 7872.
- [157] X. L. Li, P. Meduri, X. L. Chen, W. Qi, M. H. Engelhard, W. Xu, F. Ding, J. Xiao, W. Wang, C. M. Wang, J. G. Zhang, J. Liu, *J. Mater. Chem.* **2012**, *22*, 11014.
- [158] H. C. Tao, L. Z. Fan, W. L. Song, M. Wu, X. B. He, X. H. Qu, *Nanoscale* **2014**, *6*, 3138.
- [159] Y. Park, N. S. Choi, S. Park, S. H. Woo, S. Sim, B. Y. Jang, S. M. Oh, S. Park, J. Cho, K. T. Lee, *Adv. Energy Mater.* **2013**, *3*, 206.
- [160] Q. Li, Z. A. Zhang, Z. P. Guo, Y. Q. Lai, K. Zhang, J. Li, *Carbon* **2014**, *78*, 1.

- [161] X. S. Zhou, Y. X. Yin, L. J. Wan, Y. G. Guo, *Adv. Energy Mater.* **2012**, *2*, 1086.
- [162] F. F. Zhang, X. B. Zhang, Y. H. Dong, L. M. Wang, *J. Mater. Chem.* **2012**, *22*, 11452.
- [163] C. J. Chen, H. H. Xu, T. F. Zhou, Z. P. Guo, L. N. Chen, M. Y. Yan, L. Q. Mai, P. Hu, S. J. Cheng, Y. H. Huang, J. Xie, *Adv. Energy Mater.* **2016**, *6*, 1600322.
- [164] D. M. Cui, D. Tian, S. S. Chen, L. J. Yuan, *J. Mater. Chem. A* **2016**, *4*, 9177.
- [165] K. Feng, W. Ahn, G. Lui, H. W. Park, A. G. Kashkooli, G. P. Jiang, X. L. Wang, X. C. Xiao, Z. W. Chen, *Nano Energy* **2016**, *19*, 187.
- [166] X. F. Gao, J. Y. Li, D. S. Guan, C. Yuan, *ACS Appl. Mater. Interfaces* **2014**, *6*, 4154.
- [167] M. Ko, S. Chae, S. Jeong, P. Oh, J. Cho, *ACS Nano* **2014**, *8*, 8591.
- [168] T. B. Lan, H. Y. Qiu, F. Y. Xie, J. Yang, M. D. Wei, *Sci. Rep.* **2015**, *5*, 8498.
- [169] S. T. Lu, Y. W. Cheng, X. H. Wu, J. Liu, *Nano Lett.* **2013**, *13*, 2485.
- [170] Y. T. Xu, Y. Guo, C. Li, X. Y. Zhou, M. C. Tucker, X. Z. Fu, R. Sun, C. P. Wong, *Nano Energy* **2015**, *11*, 38.
- [171] Y. Yeo, J. W. Jung, K. Park, I. D. Kim, *Sci. Rep.* **2015**, *5*, 13862.
- [172] G. M. Zhou, D. W. Wang, F. Li, L. L. Zhang, N. Li, Z. S. Wu, L. Wen, G. Q. Lu, H. M. Cheng, *Chem. Mater.* **2010**, *22*, 5306.
- [173] W. Sun, R. Z. Hu, H. Liu, H. Y. Zhang, J. W. Liu, L. C. Yang, H. H. Wang, M. Zhu, *Electrochim. Acta* **2016**, *191*, 462.
- [174] H. Tang, J. Zhang, Y. J. Zhang, Q. Q. Xiong, Y. Y. Tong, Y. Li, X. L. Wang, C. D. Gu, J. P. Tu, *J. Power Sources* **2015**, *286*, 431.
- [175] Y. C. Qiu, W. F. Li, W. Zhao, G. Z. Li, Y. Hou, M. N. Liu, L. S. Zhou, F. M. Ye, H. F. Li, Z. H. Wei, S. H. Yang, W. H. Duan, Y. F. Ye, J. H. Guo, Y. G. Zhang, *Nano Lett.* **2014**, *14*, 4821.
- [176] H. L. Wang, Y. Yang, Y. Y. Liang, J. T. Robinson, Y. G. Li, A. Jackson, Y. Cui, H. J. Dai, *Nano Lett.* **2011**, *11*, 2644.
- [177] H. W. Wu, Y. Huang, M. Zong, X. Ding, J. Ding, X. Sun, *Mater. Res. Bull.* **2015**, *64*, 12.
- [178] D. H. Nagaraju, M. Kueza, G. S. Suresh, *J. Mater. Sci.* **2015**, *50*, 4244.
- [179] J. R. He, Y. F. Chen, P. J. Li, F. Fu, J. B. Liu, Z. G. Wang, *RSC Adv.* **2015**, *5*, 80063.
- [180] D. Bresser, S. Passerini, B. Scrosati, *Chem. Commun.* **2013**, *49*, 10545.
- [181] Y. Shi, J. Zhang, A. M. Bruck, Y. M. Zhang, J. Li, E. A. Stach, K. J. Takeuchi, A. C. Marschillo, E. S. Takeuchi, G. H. Yu, *Adv. Mater.* **2017**, *29*, 1603922.
- [182] S. J. Park, H. Zhao, G. Ai, C. Wang, X. Y. Song, N. Yuca, V. S. Battaglia, W. L. Yang, G. Liu, *J. Am. Chem. Soc.* **2015**, *137*, 2565.
- [183] G. Liu, S. D. Xun, N. Vukmirovic, X. Y. Song, P. Olalde-Velasco, H. H. Zheng, V. S. Battaglia, L. W. Wang, W. L. Yang, *Adv. Mater.* **2011**, *23*, 4679.
- [184] N. D. Trinh, M. Saulnier, D. Lepage, S. B. Schougaard, *J. Power Sources* **2013**, *221*, 284.
- [185] S. D. Xun, X. Y. Song, V. Battaglia, G. Liu, *J. Electrochem. Soc.* **2013**, *160*, A849.
- [186] J. M. Kim, H. S. Park, J. H. Park, T. H. Kim, H. K. Song, S. Y. Lee, *ACS Appl. Mater. Interfaces* **2014**, *6*, 12789.
- [187] H. Zhao, Y. Wei, R. M. Qiao, C. H. Zhu, Z. Y. Zheng, M. Ling, Z. Jia, Y. Bai, Y. B. Fu, J. L. Lei, X. Y. Song, V. S. Battaglia, W. L. Yang, P. B. Messersmith, G. Liu, *Nano Lett.* **2015**, *15*, 7927.
- [188] H. Zhao, A. Du, M. Ling, V. Battaglia, G. Liu, *Electrochim. Acta* **2016**, *209*, 159.
- [189] Y. Shi, X. Y. Zhou, G. H. Yu, *Acc. Chem. Res.* **2017**, *50*, 2642.
- [190] Y. N. Sun, H. Dong, Y. L. Xu, Y. Zhang, C. J. Zhao, D. Wang, Z. Liu, D. Liu, *Electrochim. Acta* **2017**, *246*, 106.
- [191] B. Song, F. Wu, Y. T. Zhu, Z. X. Hou, K. S. Moon, C. P. Wong, *Electrochim. Acta* **2018**, *267*, 213.
- [192] M. Zheng, Y. Wang, J. Reeve, H. Souzandeh, W.-H. Zhong, *Energy Storage Mater.* **2018**, *14*, 149.
- [193] Y. K. Jeong, T. W. Kwon, I. Lee, T. S. Kim, A. Coskun, J. W. Choi, *Nano Lett.* **2014**, *14*, 864.
- [194] M. H. Ryou, J. Kim, I. Lee, S. Kim, Y. K. Jeong, S. Hong, J. H. Ryu, T. S. Kim, J. K. Park, H. Lee, J. W. Choi, *Adv. Mater.* **2013**, *25*, 1571.
- [195] D. Guy, B. Lestriez, R. Bouchet, D. Guyomard, *J. Electrochem. Soc.* **2006**, *153*, A679.
- [196] I. Kovalenko, B. Zdyrko, A. Magasinski, B. Hertzberg, Z. Milicev, R. Burtovyy, I. Luginov, G. Yushin, *Science* **2011**, *334*, 75.
- [197] Q. R. Shi, L. X. Xue, Z. B. Wei, F. Liu, X. D. Du, D. D. DesMarteau, *J. Mater. Chem. A* **2013**, *1*, 15016.
- [198] J. Liu, D. G. D. Galpaya, L. J. Yan, M. H. Sun, Z. Lin, C. Yan, C. D. Liang, S. Q. Zhang, *Energy Environ. Sci.* **2017**, *10*, 750.
- [199] C. Wang, H. Wu, Z. Chen, M. T. McDowell, Y. Cui, Z. A. Bao, *Nat. Chem.* **2013**, *5*, 1042.
- [200] H. Wang, Y. Yang, L. Guo, *Adv. Energy Mater.* **2017**, *7*, 1601709.
- [201] J. Lopez, Z. Chen, C. Wang, S. C. Andrews, Y. Cui, Z. N. Bao, *ACS Appl. Mater. Interfaces* **2016**, *8*, 2318.
- [202] Z. Chen, C. Wang, J. Lopez, Z. D. Lu, Y. Cui, Z. A. Bao, *Adv. Energy Mater.* **2015**, *5*, 1401826.
- [203] T. W. Kwon, Y. K. Jeong, I. Lee, T. S. Kim, J. W. Choi, A. Coskun, *Adv. Mater.* **2014**, *26*, 7979.
- [204] X. L. Chen, W. Z. Lu, C. Chen, M. Z. Xue, *Int. J. Electrochem. Sci.* **2018**, *13*, 296.
- [205] L. J. Yan, K. Wang, S. Luo, H. C. Wu, Y. F. Luo, Y. Yu, K. L. Jiang, Q. Q. Li, S. S. Fan, J. P. Wang, *J. Mater. Chem. A* **2017**, *5*, 4047.
- [206] B. Gangaja, K. S. Reddy, S. Nair, D. Santhanagopalan, *ChemistrySelect* **2017**, *2*, 9772.
- [207] D. Zhao, Y. L. Feng, Y. G. Wang, Y. Y. Xia, *Electrochim. Acta* **2013**, *88*, 632.
- [208] A. Tolosa, S. Fleischmann, I. Grobelsek, A. Quade, E. Lim, V. Presser, *ChemSusChem* **2018**, *11*, 159.
- [209] L. L. Zhang, Z. Li, X. L. Yang, X. K. Ding, Y. X. Zhou, H. B. Sun, H. C. Tao, L. Y. Xiong, Y. H. Huang, *Nano Energy* **2017**, *34*, 111.
- [210] X. X. Li, J. J. Fu, Z. G. Pan, J. J. Su, J. W. Xu, B. Gao, X. Peng, L. Wang, X. M. Zhang, P. K. Chu, *J. Power Sources* **2016**, *331*, 58.
- [211] T. Kowase, K. Hori, K. Hasegawa, T. Momma, S. Noda, *J. Power Sources* **2017**, *363*, 450.
- [212] X. Y. Yue, W. Sun, J. Zhang, F. Wang, K. N. Sun, *J. Power Sources* **2016**, *329*, 422.
- [213] W. S. Kim, J. Choi, S. H. Hong, *Nano Res.* **2016**, *9*, 2174.
- [214] Y. H. Huang, Q. Bao, B. H. Chen, J. G. Duh, *Small* **2015**, *11*, 2314.
- [215] W. Wang, I. Ruiz, K. Ahmed, H. H. Bay, A. S. George, J. Wang, J. Butler, M. Ozkan, C. S. Ozkan, *Small* **2014**, *10*, 3389.
- [216] H. G. Zhang, P. V. Braun, *Nano Lett.* **2012**, *12*, 2778.
- [217] J. Y. Liu, H. G. Zhang, J. J. Wang, J. Cho, J. H. Pikul, E. S. Epstein, X. J. Huang, J. H. Liu, W. P. King, P. V. Braun, *Adv. Mater.* **2014**, *26*, 7096.
- [218] W. S. Chae, D. Van Gough, S. K. Ham, D. B. Robinson, P. V. Braun, *ACS Appl. Mater. Interfaces* **2012**, *4*, 3973.
- [219] J. Y. Liu, Q. Y. Zheng, M. D. Goodman, H. Y. Zhu, J. Kim, N. A. Krueger, H. L. Ning, X. J. Huang, J. H. Liu, M. Terrones, P. V. Braun, *Adv. Mater.* **2016**, *28*, 7696.
- [220] H. L. Ning, J. H. Pikul, R. Y. Zhang, X. J. Li, S. Xu, J. J. Wang, J. A. Rogers, W. P. King, P. V. Braun, *Proc. Natl. Acad. Sci. USA* **2015**, *112*, 6573.
- [221] J. Y. Liu, X. Chen, J. Kim, Q. Y. Zheng, H. L. Ning, P. C. Sun, X. J. Huang, J. H. Liu, J. J. Niu, P. V. Braun, *Nano Lett.* **2016**, *16*, 4501.
- [222] J. H. Pikul, H. G. Zhang, J. Cho, P. V. Braun, W. P. King, *Nat. Commun.* **2013**, *4*, 1732.
- [223] N. Cirigliano, G. Sun, D. Membreno, P. Malati, C. J. Kim, B. Dunn, *Energy Technol.* **2014**, *2*, 362.
- [224] J. W. Long, B. Dunn, D. R. Rolison, H. S. White, *Chem. Rev.* **2004**, *104*, 4463.

- [225] T. S. Arthur, D. J. Bates, N. Cirigliano, D. C. Johnson, P. Malati, J. M. Mosby, E. Perre, M. T. Rawls, A. L. Prieto, B. Dunn, *MRS Bull.* **2011**, 36, 523.
- [226] M. R. Lukatskaya, B. Dunn, Y. Gogotsi, *Nat. Commun.* **2016**, 7, 12647.
- [227] D. R. Rolison, J. W. Long, J. C. Lytle, A. E. Fischer, C. P. Rhodes, T. M. McEvoy, M. E. Bourga, A. M. Lubers, *Chem. Soc. Rev.* **2009**, 38, 226.
- [228] X. Huang, H. Yu, J. Chen, Z. Y. Lu, R. Yazami, H. H. Hng, *Adv. Mater.* **2014**, 26, 1296.
- [229] S. Y. Li, W. H. Xie, L. L. Gu, Z. J. Liu, X. Y. Hou, B. L. Liu, Q. Wang, D. Y. He, *Electrochim. Acta* **2016**, 193, 246.
- [230] X. H. Huang, J. P. Tu, Z. Y. Zeng, J. Y. Xiang, X. B. Zhao, *J. Electrochem. Soc.* **2008**, 155, A438.
- [231] X. J. Lin, Y. S. Shang, L. Y. Li, A. S. Yu, *ACS Sustainable Chem. Eng.* **2015**, 3, 903.
- [232] D. L. Ma, X. M. Shi, A. M. Hu, *Nanomaterials* **2016**, 6, 218.
- [233] X. B. Wang, Y. Yan, B. Hao, G. Chen, *ACS Appl. Mater. Interfaces* **2013**, 5, 3631.
- [234] L. Luo, S. H. Chung, C. H. Chang, A. Manthiram, *J. Mater. Chem. A* **2017**, 5, 15002.
- [235] D. P. Cai, H. Huang, D. D. Wang, B. Liu, L. L. Wang, Y. Liu, Q. H. Li, T. H. Wang, *ACS Appl. Mater. Interfaces* **2014**, 6, 15905.
- [236] Y. Y. Fu, X. Lu, W. K. Zhao, Y. X. Zhang, Y. H. Yang, H. L. Quan, X. T. Xu, F. Wang, *Appl. Surf. Sci.* **2015**, 357, 2013.
- [237] S. Khamlich, Z. Abdullaeva, J. V. Kennedy, M. Maaza, *Appl. Surf. Sci.* **2017**, 405, 329.
- [238] L. Zhang, K. N. Hui, K. S. Hui, H. Lee, *J. Power Sources* **2016**, 318, 76.
- [239] V. C. Tran, S. Sahoo, J. J. Shim, *Mater. Lett.* **2018**, 210, 105.
- [240] P. Wu, D. Wang, J. Ning, J. C. Zhang, X. Feng, J. G. Dong, Y. Hao, *J. Alloys Compd.* **2018**, 731, 1063.
- [241] H. X. Chen, Q. B. Zhang, X. Han, J. J. Cai, M. L. Liu, Y. Yang, K. L. Zhang, *J. Mater. Chem. A* **2015**, 3, 24022.
- [242] J. Q. Tian, Z. C. Xing, Q. X. Chu, Q. Liu, A. M. Asiri, A. H. Qusti, A. O. Al-Youbi, X. P. Sun, *CrystEngComm* **2013**, 15, 8300.
- [243] H. R. Jung, E. J. Kim, Y. J. Park, H. C. Shin, *J. Power Sources* **2011**, 196, 5122.
- [244] L. Qiao, X. L. Sun, Z. B. Yang, X. H. Wang, Q. Wang, D. Y. He, *Carbon* **2013**, 54, 29.
- [245] S. Y. Wang, G. K. Wang, X. Zhang, Y. L. Tang, J. W. Wu, X. Xiang, X. T. Zu, Q. K. Yu, *Carbon* **2017**, 120, 103.
- [246] P. Sivasakthi, G. N. K. R. Babu, K. Murugavel, S. Mohan, *J. Alloys Compd.* **2017**, 709, 240.
- [247] D. He, G. D. Wang, G. L. Liu, J. H. Bai, H. Suo, C. Zhao, *J. Alloys Compd.* **2017**, 699, 706.
- [248] F. Dogan, L. D. Sanjeeva, S. J. Hwu, J. T. Vaughey, *Solid State Ionics* **2016**, 288, 204.
- [249] H. H. Nan, W. Q. Ma, Q. Q. Hu, X. J. Zhang, *Appl. Phys. A* **2015**, 119, 1451.
- [250] D. Mazouzi, D. Reyter, M. Gauthier, P. Moreau, D. Guyomard, L. Roue, B. Lestriez, *Adv. Energy Mater.* **2014**, 4, 1301718.
- [251] S. Eugenio, T. M. Silva, M. J. Carmezim, R. G. Duarte, M. F. Montemor, *J. Appl. Electrochem.* **2014**, 44, 455.
- [252] X. F. Wei, Y. B. Guan, X. H. Zheng, Q. Z. Zhu, J. R. Shen, N. Qiao, S. Q. Zhou, B. Xu, *Appl. Surf. Sci.* **2018**, 440, 748.
- [253] Y. Feng, Y. L. Zhang, X. Y. Song, Y. Z. Wei, V. S. Battaglia, *Sustainable Energy Fuels* **2017**, 1, 767.
- [254] H. H. Wang, S. T. Lu, Y. Chen, L. Han, J. Zhou, X. H. Wu, W. Qin, *J. Mater. Chem. A* **2015**, 3, 23677.
- [255] A. K. Rai, J. Gim, S. W. Kang, V. Mathew, L. T. Anh, J. Kang, J. Song, B. J. Paul, J. Kim, *Mater. Chem. Phys.* **2012**, 136, 1044.
- [256] P. Guo, H. Song, X. Chen, L. Ma, G. Wang, F. Wang, *Anal. Chim. Acta* **2011**, 688, 146.
- [257] S. Z. Huang, Y. Li, Y. Y. Feng, H. R. An, P. Long, C. Q. Qin, W. Feng, *J. Mater. Chem. A* **2015**, 3, 23095.
- [258] C. L. Ma, Y. Zhao, Y. Li, *Chem. Eng. J.* **2017**, 320, 283.
- [259] H. Y. Sun, A. E. D. Castillo, S. Monaco, A. Capasso, A. Ansaldo, M. Prato, D. A. Dinh, V. Pellegrini, B. Scrosati, L. Manna, F. Bonaccorso, *J. Mater. Chem. A* **2016**, 4, 6886.
- [260] Y. S. Yun, Y. U. Park, S. J. Chang, B. H. Kim, J. Choi, J. J. Wang, D. Zhang, P. V. Braun, H. J. Jin, K. Kang, *Carbon* **2016**, 99, 658.
- [261] H. S. Li, Y. Ding, H. Ha, Y. Shi, L. L. Peng, X. G. Zhang, C. J. Ellison, G. H. Yu, *Adv. Mater.* **2017**, 29, 1700898.
- [262] N. Li, Z. P. Chen, W. C. Ren, F. Li, H. M. Cheng, *Proc. Natl. Acad. Sci. USA* **2012**, 109, 17360.
- [263] X. H. Rui, W. P. Sun, C. Wu, Y. Yu, Q. Y. Yan, *Adv. Mater.* **2015**, 27, 6670.
- [264] C. Zhang, T. Kuila, N. H. Kim, S. H. Lee, J. H. Lee, *Carbon* **2015**, 89, 328.
- [265] A. Bello, F. Barzegar, D. Momodu, J. Dangbegnon, F. Taghizadeh, M. Fabiane, N. Manyala, *J. Power Sources* **2015**, 273, 305.
- [266] Y. Zhao, J. Liu, Y. Hu, H. H. Cheng, C. G. Hu, C. C. Jiang, L. Jiang, A. Y. Cao, L. T. Qu, *Adv. Mater.* **2013**, 25, 591.
- [267] X. C. Dong, X. W. Wang, L. Wang, H. Song, X. G. Li, L. H. Wang, M. B. Chan-Park, C. M. Li, P. Chen, *Carbon* **2012**, 50, 4865.
- [268] L. F. Shen, X. G. Zhang, E. Uchaker, C. Z. Yuan, G. Z. Cao, *Adv. Energy Mater.* **2012**, 2, 691.
- [269] C. J. Chen, Y. Zhang, Y. J. Li, Y. D. Kuang, J. W. Song, W. Luo, Y. B. Wang, Y. G. Yao, G. Pastel, J. Xie, L. B. Hu, *Adv. Energy Mater.* **2017**, 7, 1700595.
- [270] W. Yuan, B. Y. Wang, H. Wu, M. W. Xiang, Q. Wang, H. Liu, Y. Zhang, H. K. Liu, S. X. Dou, *J. Power Sources* **2018**, 379, 10.
- [271] G. R. Sun, Q. Zhao, T. Wu, W. Lu, M. Bao, L. Q. Sun, H. M. Xie, J. Liu, *ACS Appl. Mater. Interfaces* **2018**, 10, 6327.
- [272] S. Y. Chu, Y. J. Zhong, R. Cai, Z. B. Zhang, S. Y. Wei, Z. P. Shao, *Small* **2016**, 12, 6724.
- [273] S. Jeong, S. An, J. Jeong, J. Lee, Y. Kwon, *J. Power Sources* **2015**, 278, 245.
- [274] M. Depardieu, R. Janot, C. Sanchez, A. Bentaleb, R. Demir-Cakan, C. Gervais, M. Birot, M. Morcrette, R. Backov, *J. Mater. Chem. A* **2014**, 2, 18047.
- [275] S. Jun, S. H. Joo, R. Ryoo, M. Kruk, M. Jaroniec, Z. Liu, T. Ohsuna, O. Terasaki, *J. Am. Chem. Soc.* **2000**, 122, 10712.
- [276] H. B. Yao, G. Y. Zheng, W. Y. Li, M. T. McDowell, Z. W. Seh, N. A. Liu, Z. D. Lu, Y. Cui, *Nano Lett.* **2013**, 13, 3385.
- [277] A. Volperts, G. Dobe, A. Zhurinsk, D. Vervikishko, E. Shkolnikov, J. Ozolinsh, *New Carbon Mater.* **2017**, 32, 319.
- [278] J. R. Luo, X. H. Yao, L. Yang, Y. Han, L. Chen, X. M. Geng, V. Vattipalli, Q. Dong, W. Fan, D. W. Wang, H. L. Zhu, *Nano Res.* **2017**, 10, 4318.
- [279] J. Z. Chen, X. Y. Zhou, C. T. Mei, J. L. Xu, S. Zhou, C. P. Wong, *J. Power Sources* **2017**, 342, 48.
- [280] C. J. Chen, Y. Zhang, Y. J. Li, J. Q. Dai, J. W. Song, Y. G. Yao, Y. H. Gong, I. Kierzewski, J. Xie, L. B. Hu, *Energy Environ. Sci.* **2017**, 10, 538.
- [281] S. Y. Lyu, Y. P. Chen, S. J. Han, L. M. Guo, N. Yang, S. Q. Wang, *RSC Adv.* **2017**, 7, 54806.
- [282] A. Gutierrez-Pardo, B. Lacroix, J. Martinez-Fernandez, J. Ramirez-Rico, *ACS Appl. Mater. Interfaces* **2016**, 8, 30890.
- [283] A. Cuna, M. R. O. Vega, E. L. da Silva, N. Tancredi, C. Radtke, C. F. Malfatti, *Int. J. Hydrogen Energy* **2016**, 41, 12127.
- [284] C. C. Wan, Y. Jiao, J. Li, *RSC Adv.* **2016**, 6, 64811.
- [285] D. Liu, S. Yu, Y. L. Shen, H. Chen, Z. H. Shen, S. Y. Zhao, S. Y. Fu, Y. M. Yu, B. F. Bao, *Ind. Eng. Chem. Res.* **2015**, 54, 12570.
- [286] S. Yu, D. Liu, S. Y. Zhao, B. F. Bao, C. D. Jin, W. J. Huang, H. Chen, Z. H. Shen, *RSC Adv.* **2015**, 5, 30943.
- [287] A. Cuna, N. Tancredi, J. Bussi, V. Barranco, T. A. Centeno, A. Quevedo, J. M. Rojo, *J. Electrochem. Soc.* **2014**, 161, A1806.
- [288] J. H. Jiang, L. Zhang, X. Y. Wang, N. Holm, K. Rajagopalan, F. L. Chen, S. G. Ma, *Electrochim. Acta* **2013**, 113, 481.

- [289] Y. Wang, A. Gozen, L. Chen, W. H. Zhong, *Adv. Energy Mater.* **2017**, 7, 1601767.
- [290] Y. Wang, W. H. Zhong, T. Schiff, A. Eyler, B. Li, *Adv. Energy Mater.* **2015**, 5, 1400463.
- [291] Y. Wang, B. Li, J. Y. Ji, A. Eyler, W. H. Zhong, *Adv. Energy Mater.* **2013**, 3, 1557.
- [292] Y. H. Zou, X. F. Yang, C. X. Lv, T. C. Liu, Y. Z. Xia, L. Shang, G. I. N. Waterhouse, D. J. Yang, T. R. Zhang, *Adv. Sci.* **2017**, 4, 1600262.
- [293] S. J. Shi, Z. R. Lou, T. F. Xia, X. L. Wang, C. D. Gu, J. P. Tu, *J. Power Sources* **2014**, 257, 198.
- [294] S. Hwang, W. Chang, S. M. Kim, D. Su, D. H. Kim, J. Y. Lee, K. Y. Chung, E. A. Stach, *Chem. Mater.* **2014**, 26, 1084.
- [295] W. Bauer, D. Notzel, V. Wenzel, H. Nirschl, *J. Power Sources* **2015**, 288, 359.
- [296] N. Wongtharom, T. C. Lee, C. H. Hsu, G. T. K. Fey, K. P. Huang, J. K. Chang, *J. Power Sources* **2013**, 240, 676.
- [297] L. M. Suo, Y. S. Hu, H. Li, M. Armand, L. Q. Chen, *Nat. Commun.* **2013**, 4, 1481.
- [298] J. C. Forgie, S. El Khakani, D. D. MacNeil, D. Rochefort, *Phys. Chem. Chem. Phys.* **2013**, 15, 7713.
- [299] Y. Wang, W.-H. Zhong, *ChemElectroChem* **2015**, 2, 22.
- [300] Y. S. Zhu, S. Y. Xiao, Y. Shi, Y. Q. Yang, Y. Y. Hou, Y. P. Wu, *Adv. Energy Mater.* **2014**, 4, 1300647.
- [301] S. H. Wang, S. S. Hou, P. L. Kuo, H. Teng, *ACS Appl. Mater. Interfaces* **2013**, 5, 8477.
- [302] D. F. Miranda, C. Versek, M. T. Tuominen, T. P. Russell, J. J. Watkins, *Macromolecules* **2013**, 46, 9313.
- [303] D. T. Hallinan, S. A. Mullin, G. M. Stone, N. P. Balsara, *J. Electrochem. Soc.* **2013**, 160, A464.
- [304] E. Rangasamy, G. Sahu, J. K. Keum, A. J. Rondinone, N. J. Dudney, C. D. Liang, *J. Mater. Chem. A* **2014**, 2, 4111.
- [305] A. Hayashi, K. Noi, A. Sakuda, M. Tatsumisago, *Nat. Commun.* **2012**, 3, 856.
- [306] G. Delaizir, V. Viallet, A. Aboulaich, R. Bouchet, L. Tortet, V. Seznec, M. Morcrette, J. M. Tarascon, P. Rozier, M. Dolle, *Adv. Funct. Mater.* **2012**, 22, 2140.
- [307] N. Kamaya, K. Homma, Y. Yamakawa, M. Hirayama, R. Kanno, M. Yonemura, T. Kamiyama, Y. Kato, S. Hama, K. Kawamoto, A. Mitsui, *Nat. Mater.* **2011**, 10, 682.
- [308] J. F. Ihlefeld, P. G. Clem, B. L. Doyle, P. G. Kotula, K. R. Fenton, C. A. Appleby, *Adv. Mater.* **2011**, 23, 5663.
- [309] X. Fu, Y. Wang, J. Tuba, L. Scudiero, W.-H. Zhong, *Small Methods* **2018**, 2, 1800066.
- [310] S. W. Peterson, D. R. Wheeler, *J. Electrochem. Soc.* **2014**, 161, A2175.
- [311] T. Terao, G. Inoue, M. Kawase, N. Kubo, M. Yamaguchi, K. Yokoyama, T. Tokunaga, K. Shinohara, Y. Hara, T. Hara, *J. Power Sources* **2017**, 347, 108.
- [312] S. Muller, P. Pietsch, B. Brandt, P. Baade, V. De Andrade, F. De Carlo, V. Wood, *Nat. Commun.* **2018**, 9, 2340.
- [313] S. Lee, A. M. Sastry, J. Park, *J. Power Sources* **2016**, 315, 96.
- [314] G. Inoue, M. Kawase, *J. Power Sources* **2017**, 342, 476.
- [315] T. Danner, M. Singh, S. Hein, J. Kaiser, H. Hahn, A. Latz, *J. Power Sources* **2016**, 334, 191.
- [316] R. B. Smith, M. Z. Bazant, *J. Electrochem. Soc.* **2017**, 164, E3291.
- [317] C. P. Andersen, H. Hu, G. Qiu, V. Kalra, Y. Sun, *J. Electrochem. Soc.* **2015**, 162, A1135.
- [318] T. Carraro, J. Joos, B. Ruger, A. Weber, E. Ivers-Tiffée, *Electrochim. Acta* **2012**, 77, 315.